



# Magnetic Field Imaging at ASDEX Upgrade with the Imaging Motional Stark Effect diagnostic

IPP Fachbeirat, Garching September 2013

O. P. Ford,<sup>1</sup> J. Howard,<sup>2</sup> M. Reich,<sup>1</sup> J. Hobirk,<sup>1</sup>  
J. Svensson,<sup>1</sup> R. Wolf,<sup>1</sup> ASDEX Upgrade Team

1: Max-Planck Institut für Plasmaphysik, Greifswald/Garching, Germany

2: Plasma Research Laboratory, Australian National University, Canberra



# Motivation: Current Tomography from 2D measurements

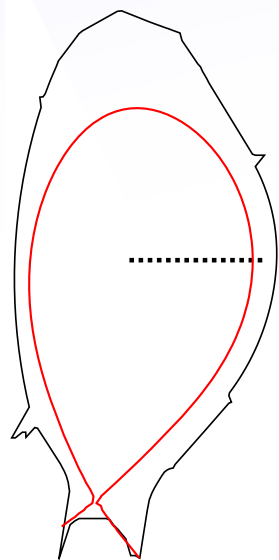
Magnetic configuration and current distribution are very important for many aspects of Tokamak physics. Various diagnostics give constraints on the magnetic field  $B_z$ .

# Motivation: Current Tomography from 2D measurements

Magnetic configuration and current distribution are very important for many aspects of Tokamak physics. Various diagnostics give constraints on the magnetic field  $B_z$ .

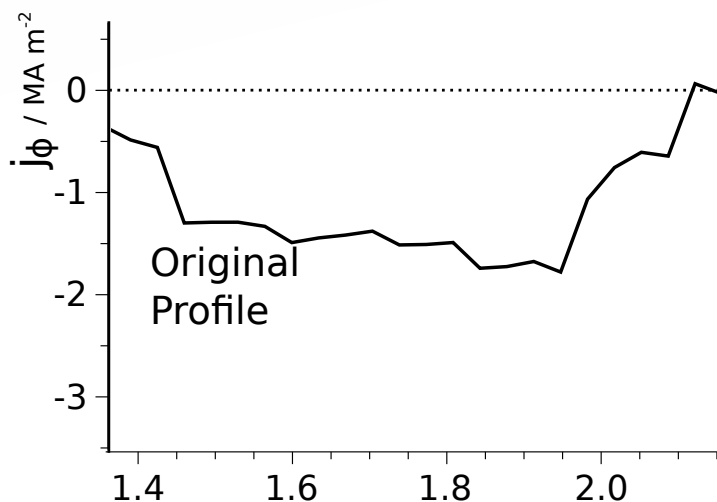
Tomographic reconstructions of ASDEX Upgrade current from simulated external magnetic sensors and magnetic pitch angle measurements reveal that the current profile is more constrained by a distributed 2D grid of data points, than the same amount of data on the conventional 1D line.

$j\phi$  Uncertainty

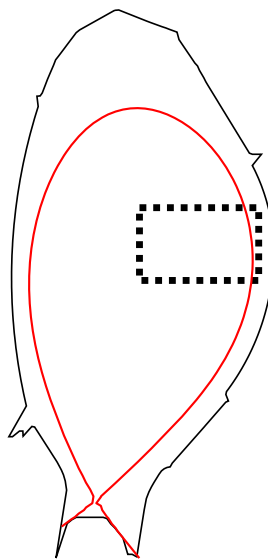


**Magnetics + MSE system:**

30 x  $B_z$  at 30 positions along NBI centre.

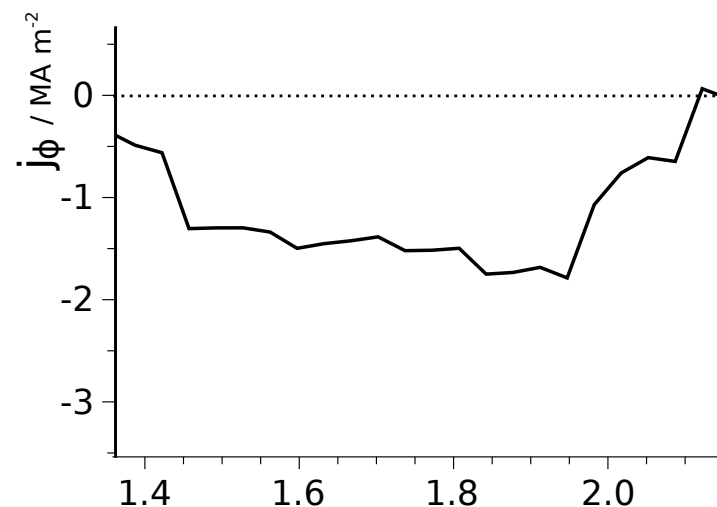


$j\phi$  Uncertainty



**Magnetics + IMSE System:**

30x30 grid of  $B_z$  measurements.



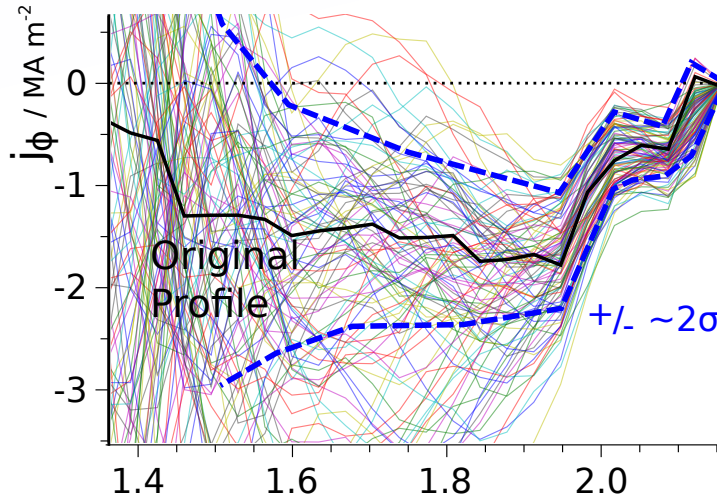
# Motivation: Current Tomography from 2D measurements

Magnetic configuration and current distribution are very important for many aspects of Tokamak physics. Various diagnostics give constraints on the magnetic field  $B_z$ .

Tomographic reconstructions of ASDEX Upgrade current from simulated external magnetic sensors and magnetic pitch angle measurements reveal that the current profile is more constrained by a distributed 2D grid of data points, than the same amount of data on the conventional 1D line.

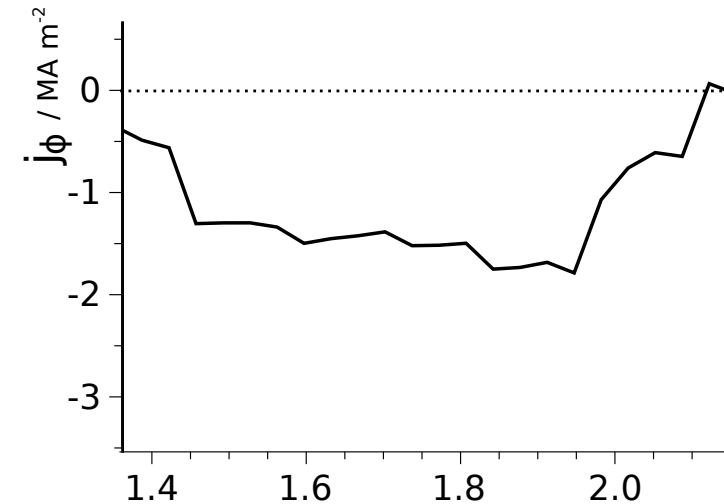
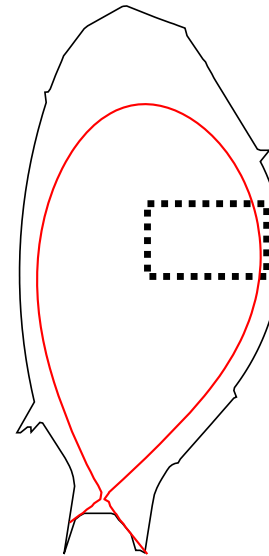
$j\phi$  Uncertainty

**Magnetics + MSE system:**  
30 x  $B_z$  at 30 positions along  
NBI centre.



$j\phi$  Uncertainty

**Magnetics + IMSE System:**  
30x30 grid of  $B_z$  measurements.

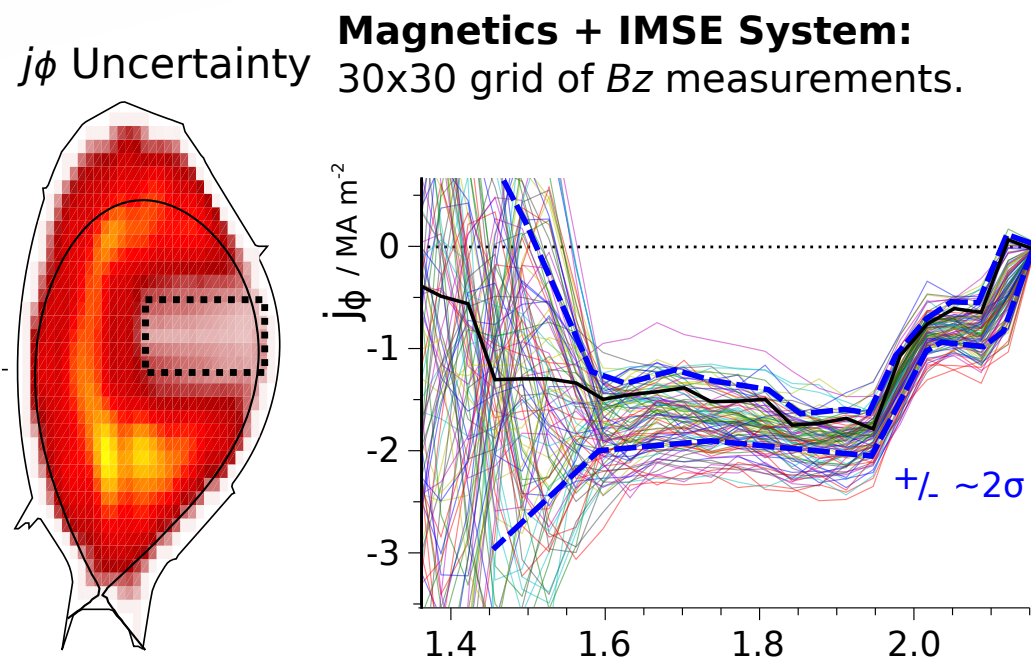
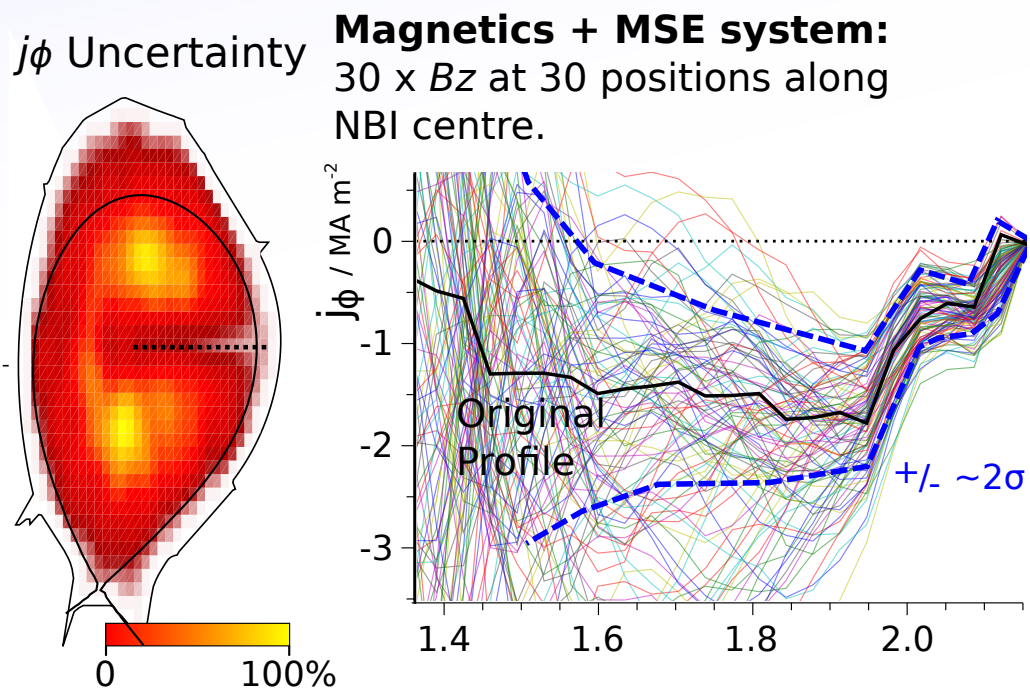


0 100%

# Motivation: Current Tomography from 2D measurements

Magnetic configuration and current distribution are very important for many aspects of Tokamak physics. Various diagnostics give constraints on the magnetic field  $B_z$ .

Tomographic reconstructions of ASDEX Upgrade current from simulated external magnetic sensors and magnetic pitch angle measurements reveal that the current profile is more constrained by a distributed 2D grid of data points, than the same amount of data on the conventional 1D line.



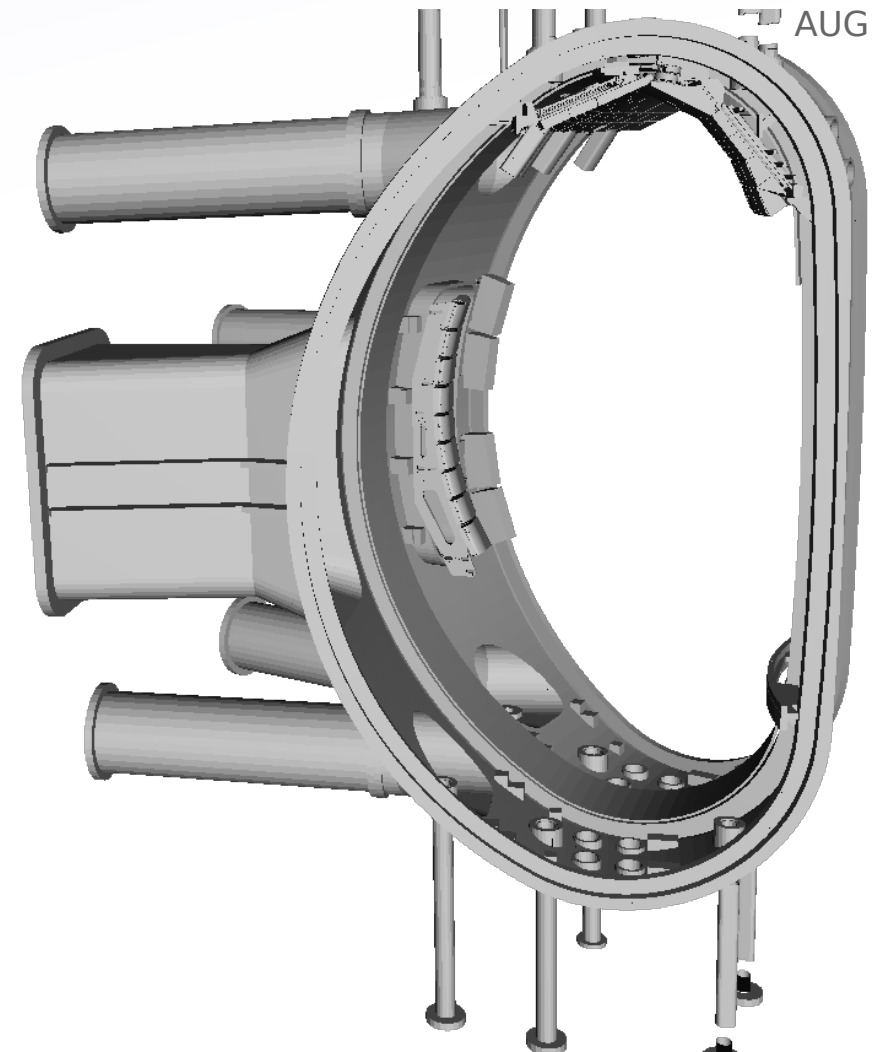
Each case has 900 measurements at  $\sigma = 10\text{mT}$ . So difference is only in the **type** of information.

**Conclusion:** 2D information greatly improves current inference ability, beyond just the increase in data quantity.



# (Imaging) Motional Stark Effect at AUG

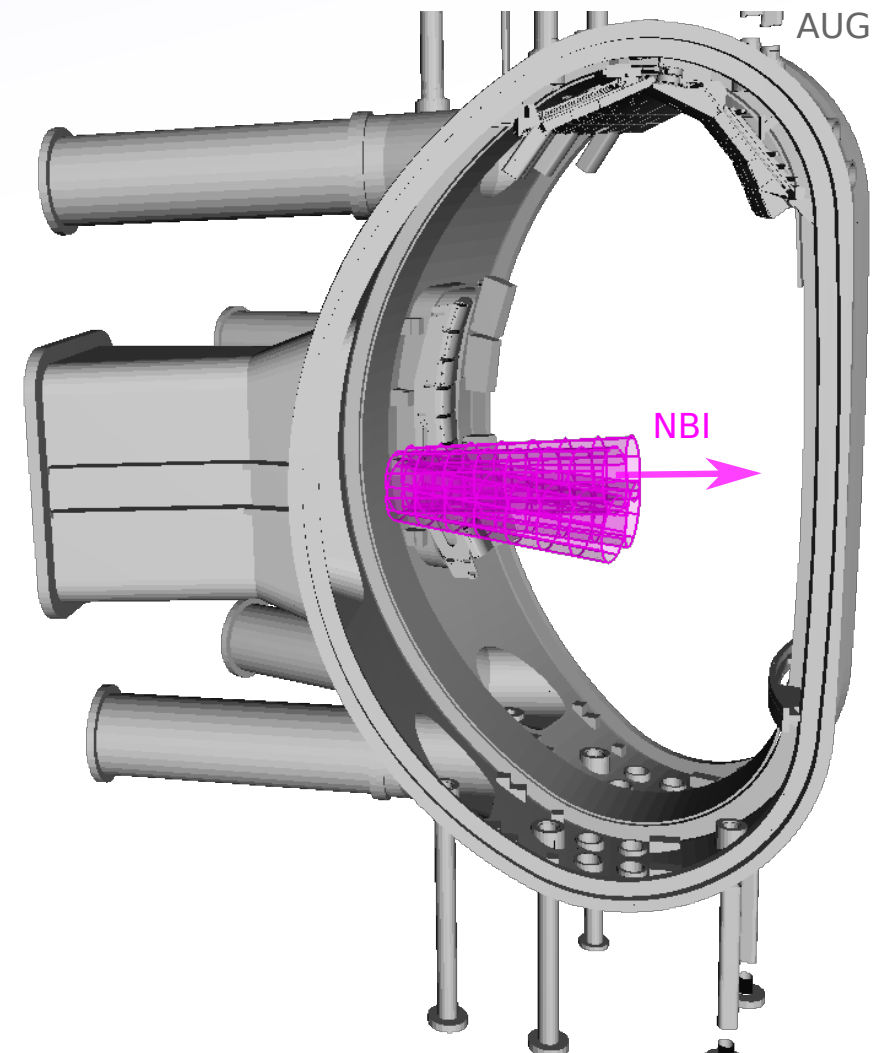
ASDEX Upgrade has an existing 10-channel MSE system.



## (Imaging) Motional Stark Effect at AUG

ASDEX Upgrade has an existing 10-channel MSE system.

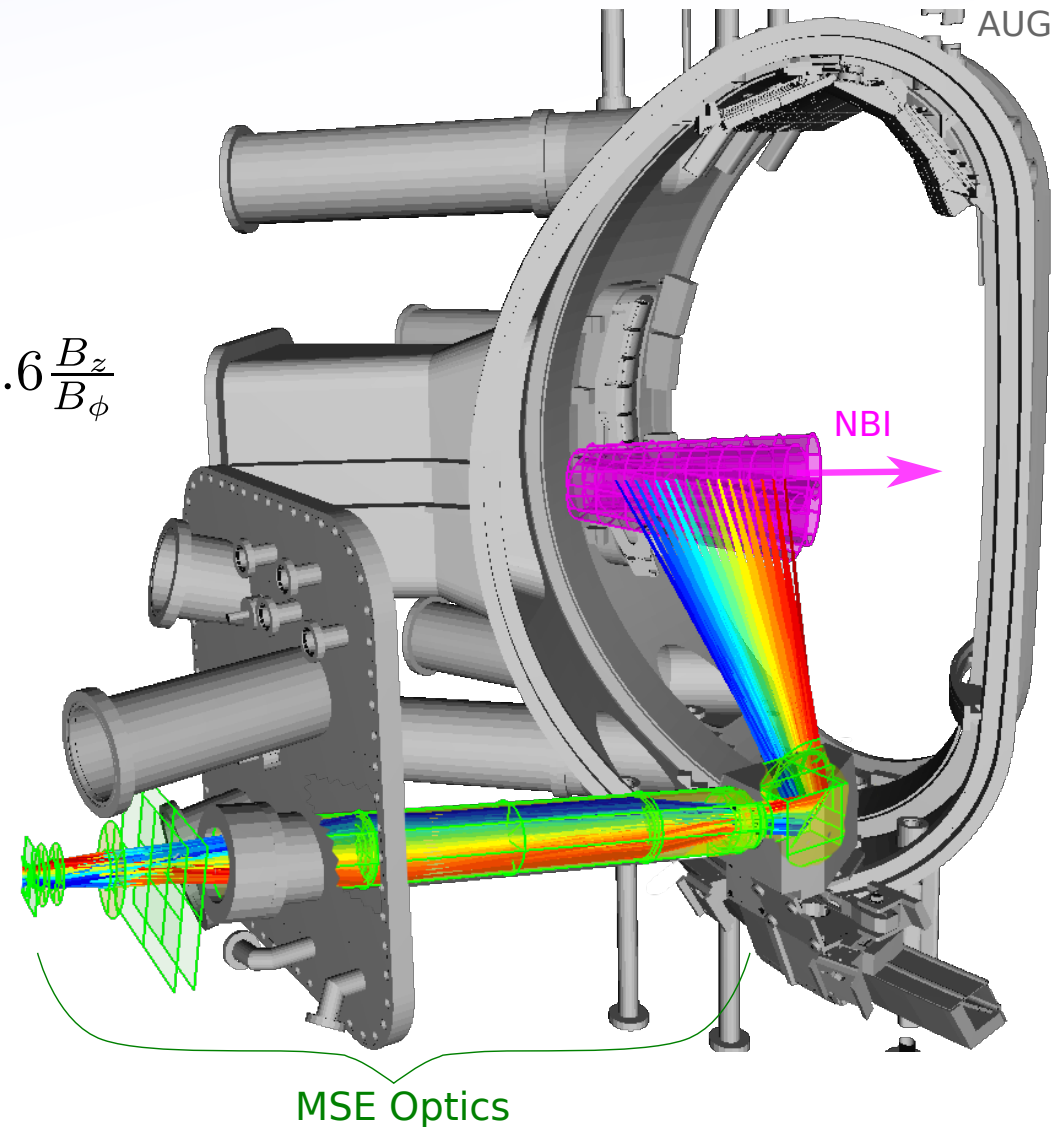
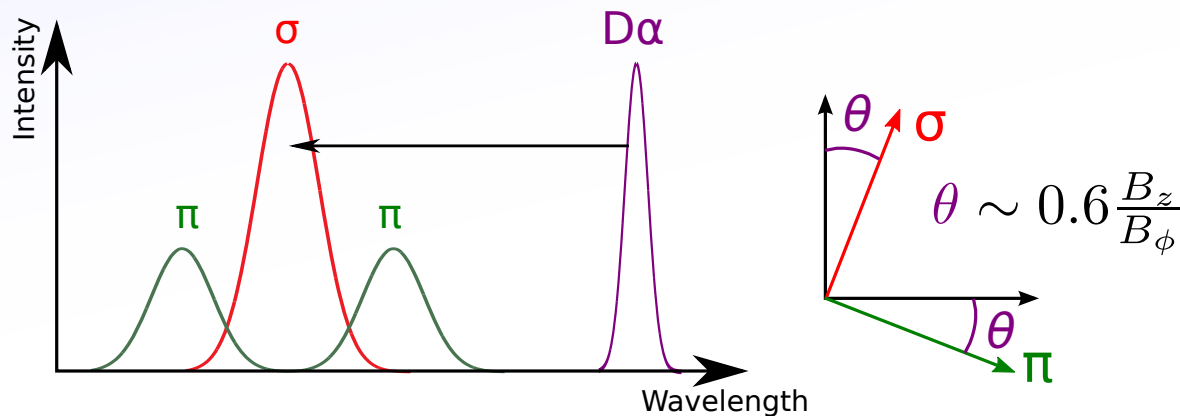
$H\alpha/D\alpha$  beam emission is Doppler shifted by beam velocity and split by the Motional Stark Effect into  $\pi$  and  $\sigma$  components which are polarised perpendicular and parallel to projected  $\mathbf{v} \times \mathbf{B}$  direction:



# (Imaging) Motional Stark Effect at AUG

ASDEX Upgrade has an existing 10-channel MSE system.

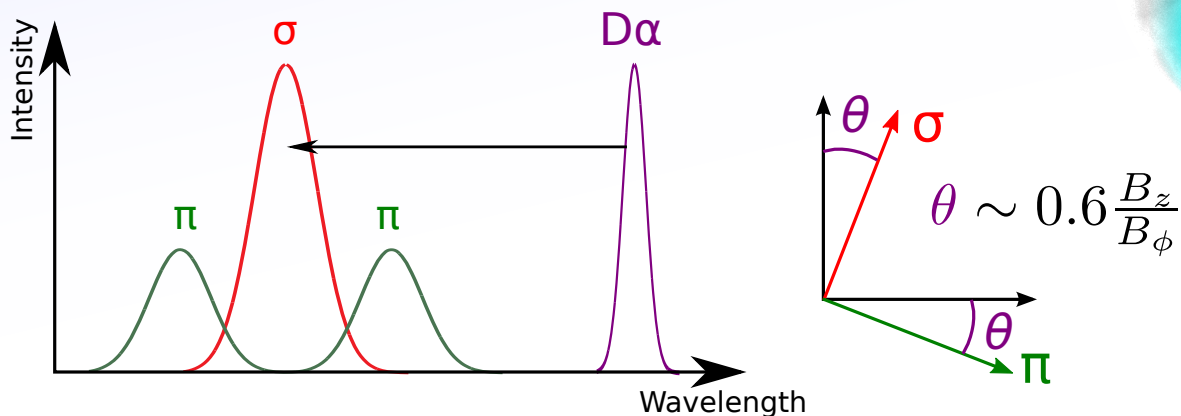
H $\alpha$ /D $\alpha$  beam emission is Doppler shifted by beam velocity and split by the Motional Stark Effect into  $\pi$  and  $\sigma$  components which are polarised perpendicular and parallel to projected  $\mathbf{v} \times \mathbf{B}$  direction:



# (Imaging) Motional Stark Effect at AUG

ASDEX Upgrade has an existing 10-channel MSE system.

H $\alpha$ /D $\alpha$  beam emission is Doppler shifted by beam velocity and split by the Motional Stark Effect into  $\pi$  and  $\sigma$  components which are polarised perpendicular and parallel to projected  $\mathbf{v} \times \mathbf{B}$  direction:



The IMSE observes a full image of the beam emission using a CCD camera, giving  $> 60 \times 60$   $\theta$  measurements.

As well as the increase in data, the 2D spread can be shown to give more information for current inference (tomographic reconstruction)

It replaced the MSE for two short periods of plasma operation this year with the objective of testing the basic principle.

Modelled Image

Conventional MSE

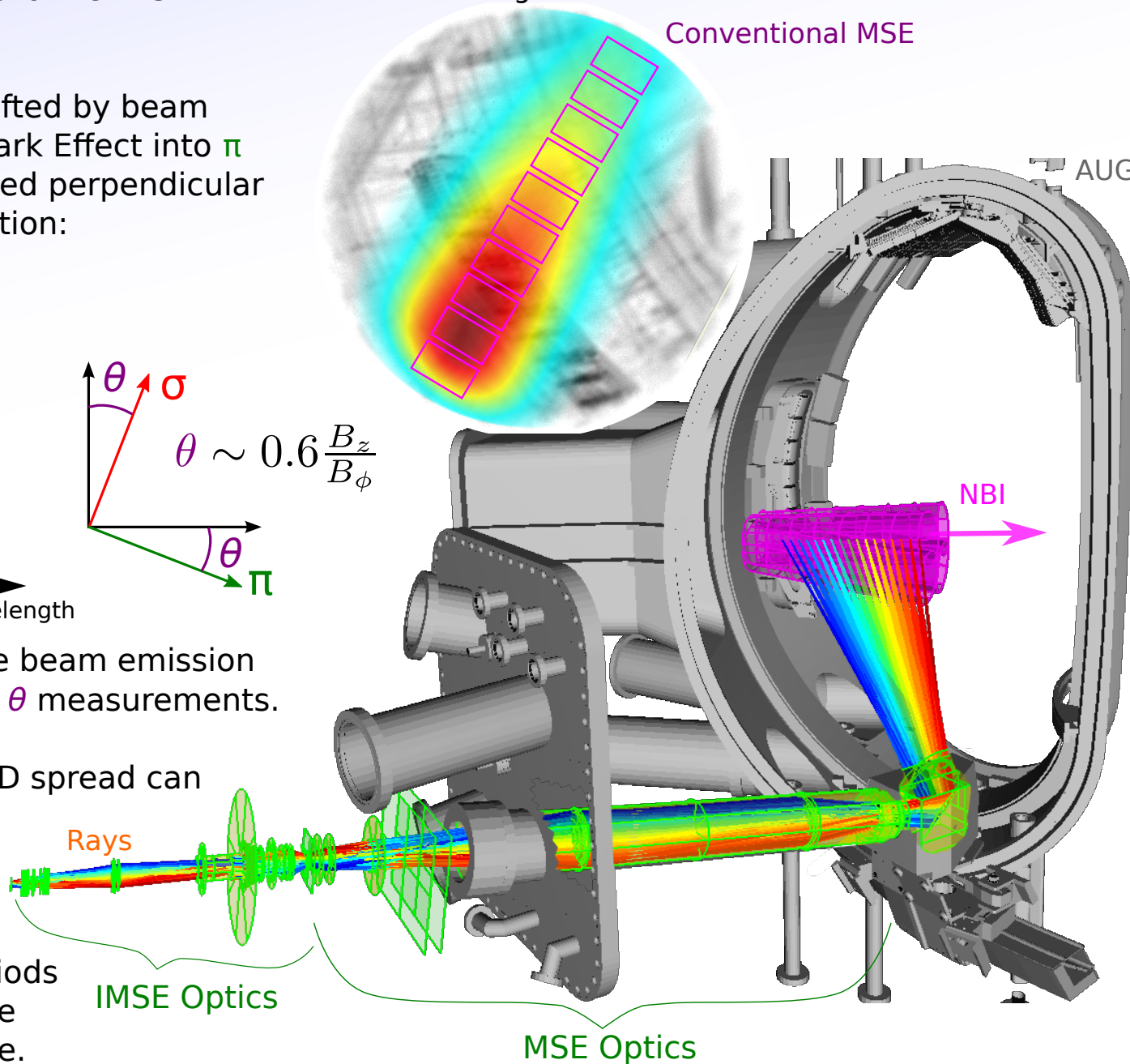
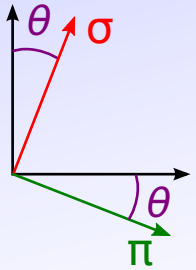


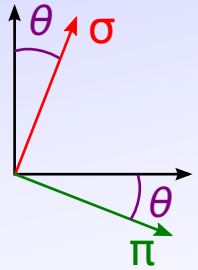
# Image Demodulation



Two birefringent plates modulate the image with orthogonal interference patterns. The difference in the wavelength of the  $\sigma$  and  $\pi$  components is exploited to cause their interference patterns to add. Since the measurement of  $\theta$  is periodic in  $90^\circ$ , the angle  $\theta$  from each of the  $\sigma$  and  $\pi$  are averaged.

(Details in P6.006 poster, Diagnostics Satellite Meeting, Saturday)

# Image Demodulation



Two birefringent plates modulate the image with orthogonal interference patterns. The difference in the wavelength of the  $\sigma$  and  $\pi$  components is exploited to cause their interference patterns to add. Since the measurement of  $\theta$  is periodic in  $90^\circ$ , the angle  $\theta$  from each of the  $\sigma$  and  $\pi$  are averaged.

(Details in P6.006 poster, Diagnostics Satellite Meeting, Saturday)

The image produced follows:

$$I \propto 1 + \zeta \cos(2\theta) \cos(x) + \zeta \sin(2\theta) \cos(x+y) + \zeta \sin(2\theta) \cos(x-y)$$

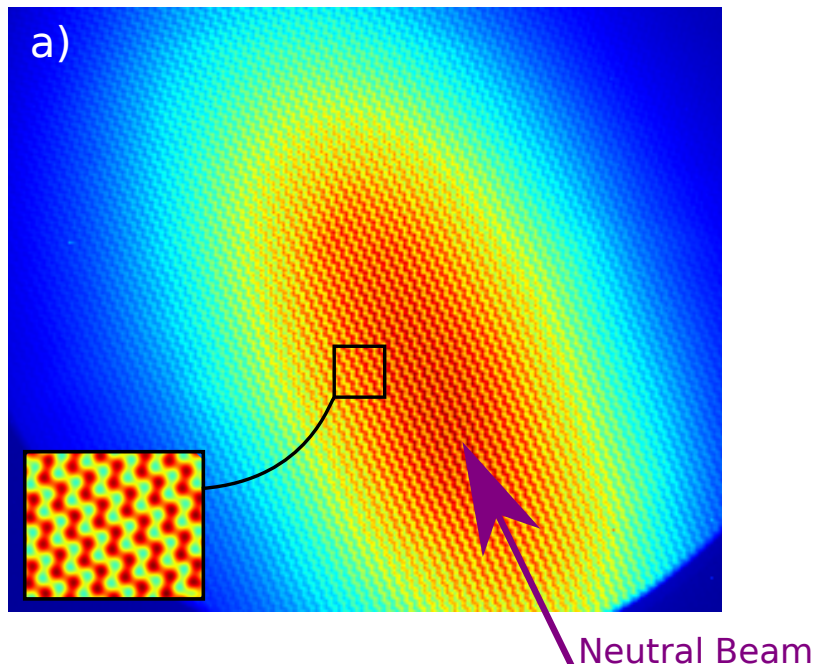
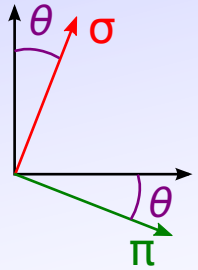


# Image Demodulation



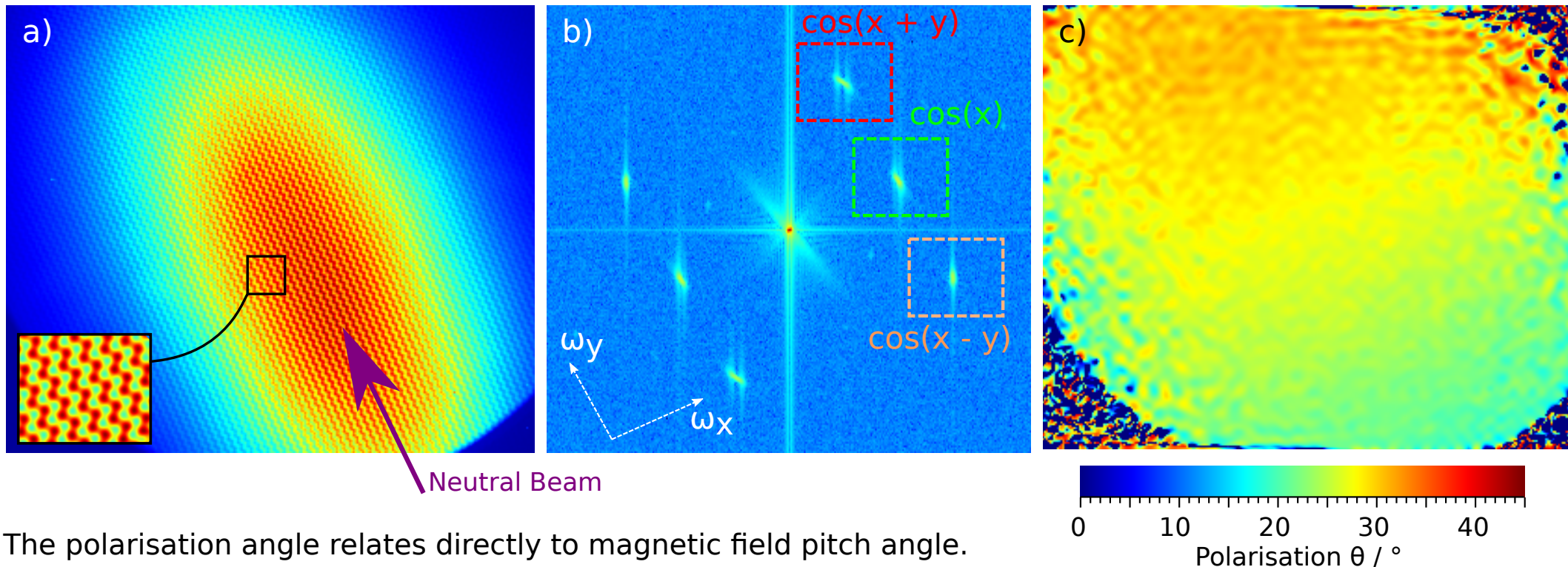
Two birefringent plates modulate the image with orthogonal interference patterns. The difference in the wavelength of the  $\sigma$  and  $\pi$  components is exploited to cause their interference patterns to add. Since the measurement of  $\theta$  is periodic in  $90^\circ$ , the angle  $\theta$  from each of the  $\sigma$  and  $\pi$  are averaged.

(Details in P6.006 poster, Diagnostics Satellite Meeting, Saturday)

The image produced follows:

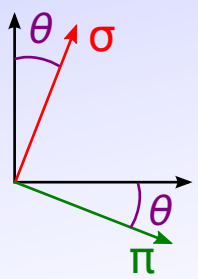
$$I \propto 1 + \zeta \cos(2\theta) \cos(x) + \zeta \sin(2\theta) \cos(x+y) + \zeta \sin(2\theta) \cos(x-y)$$

The three components can be easily isolated from the 2D Fourier Transform:



The polarisation angle relates directly to magnetic field pitch angle.

# Image Demodulation



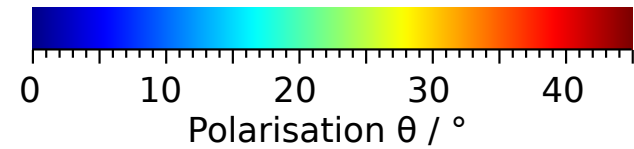
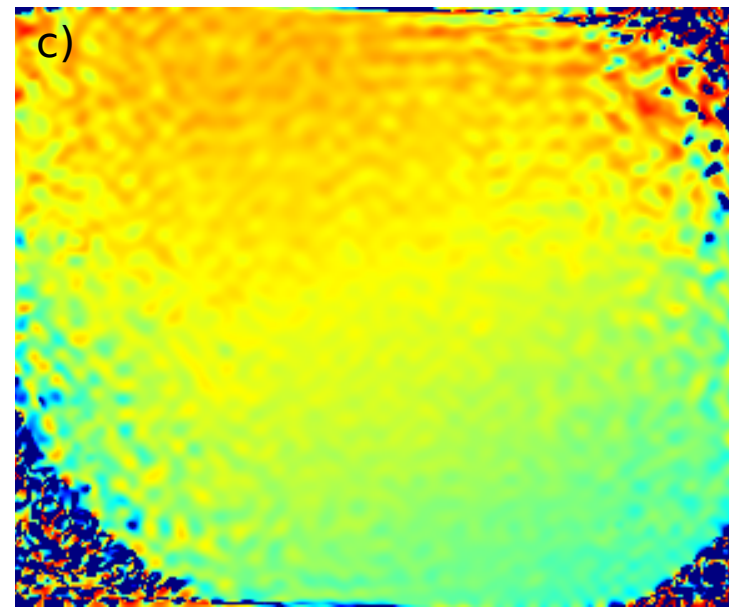
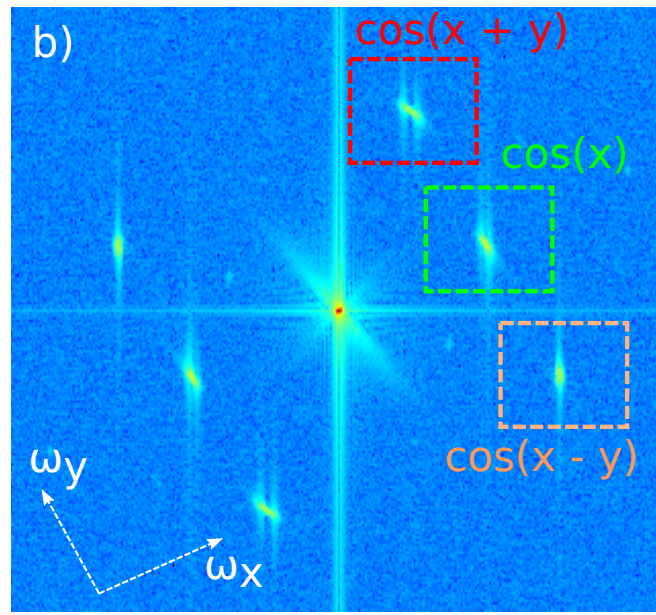
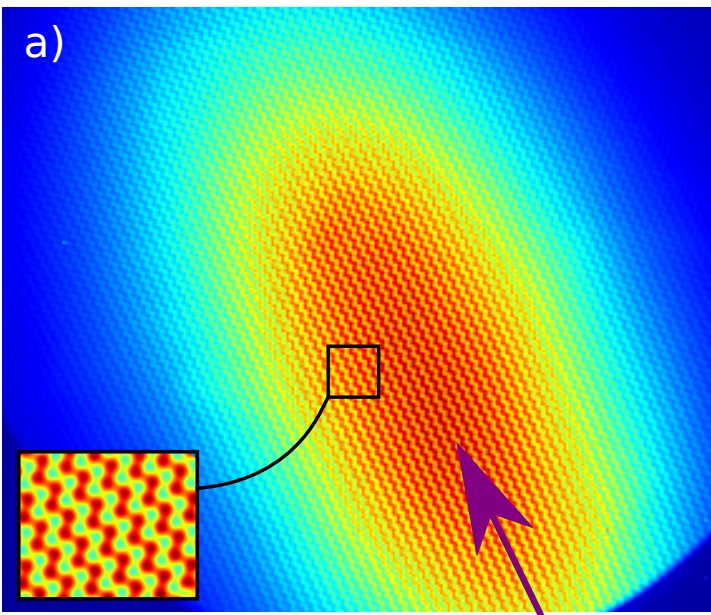
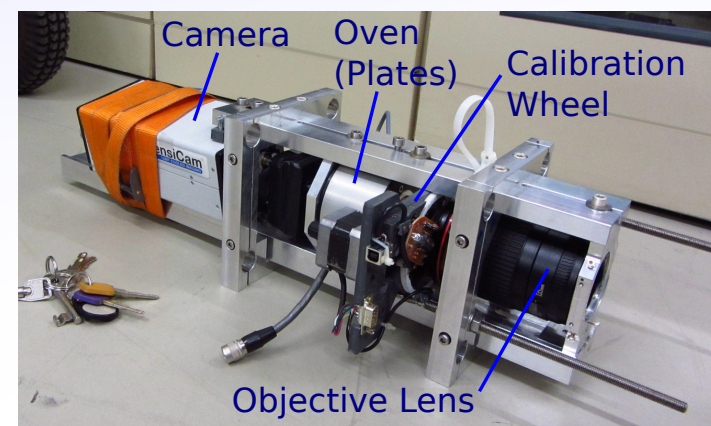
Two birefringent plates modulate the image with orthogonal interference patterns. The difference in the wavelength of the  $\sigma$  and  $\pi$  components is exploited to cause their interference patterns to add. Since the measurement of  $\theta$  is periodic in  $90^\circ$ , the angle  $\theta$  from each of the  $\sigma$  and  $\pi$  are averaged.

(Details in P6.006 poster, Diagnostics Satellite Meeting, Saturday)

The image produced follows:

$$I \propto 1 + \zeta \cos(2\theta) \cos(x) + \zeta \sin(2\theta) \cos(x+y) + \zeta \sin(2\theta) \cos(x-y)$$

The three components can be easily isolated from the 2D Fourier Transform:



The polarisation angle relates directly to magnetic field pitch angle.

# Image Transform

The imaging nature of the system allows easy position calibration by identifying known features in a background image and calculating the intersection with the neutral beam:

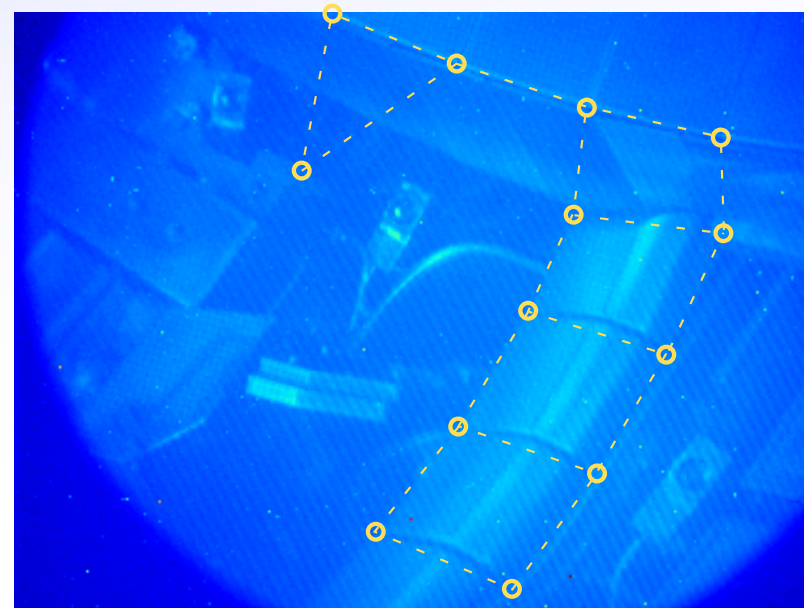
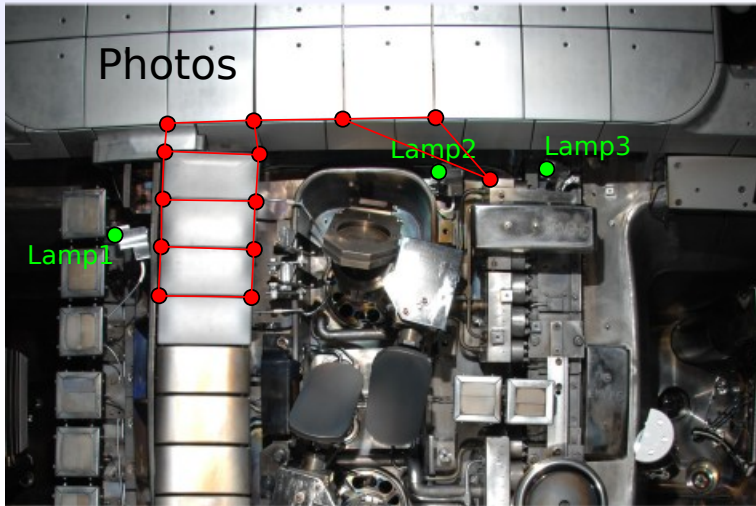
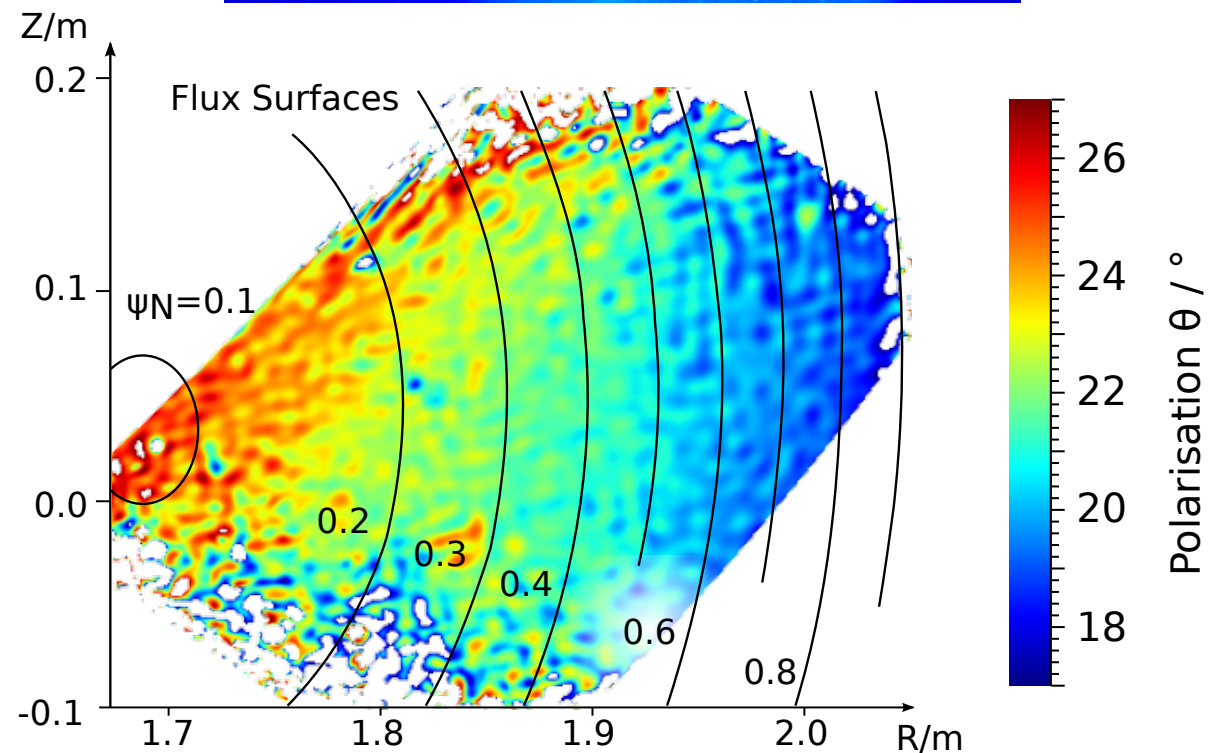
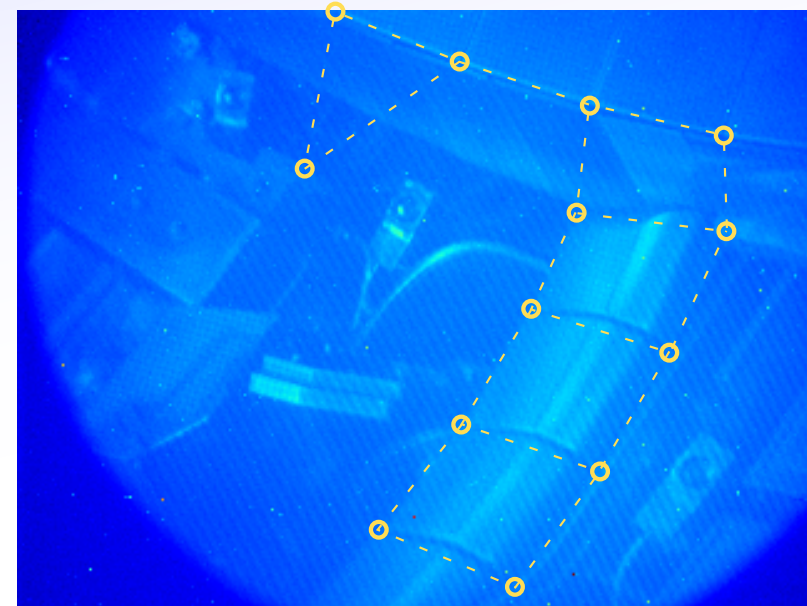
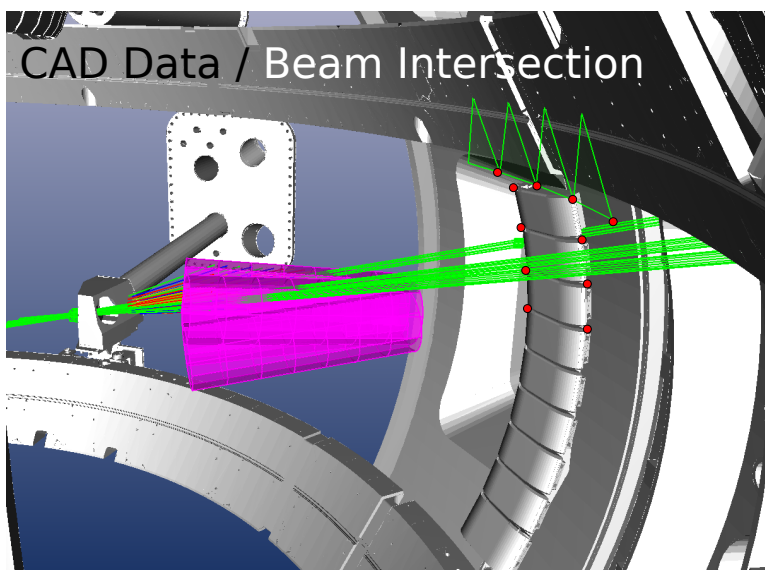
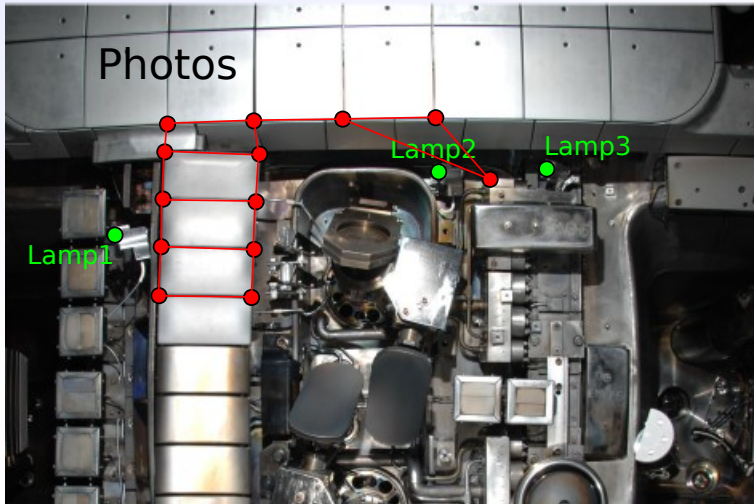


# Image Transform

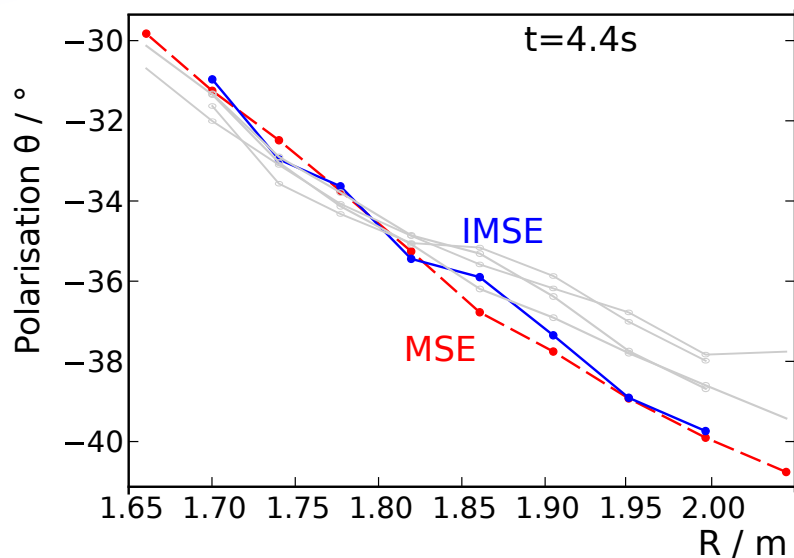
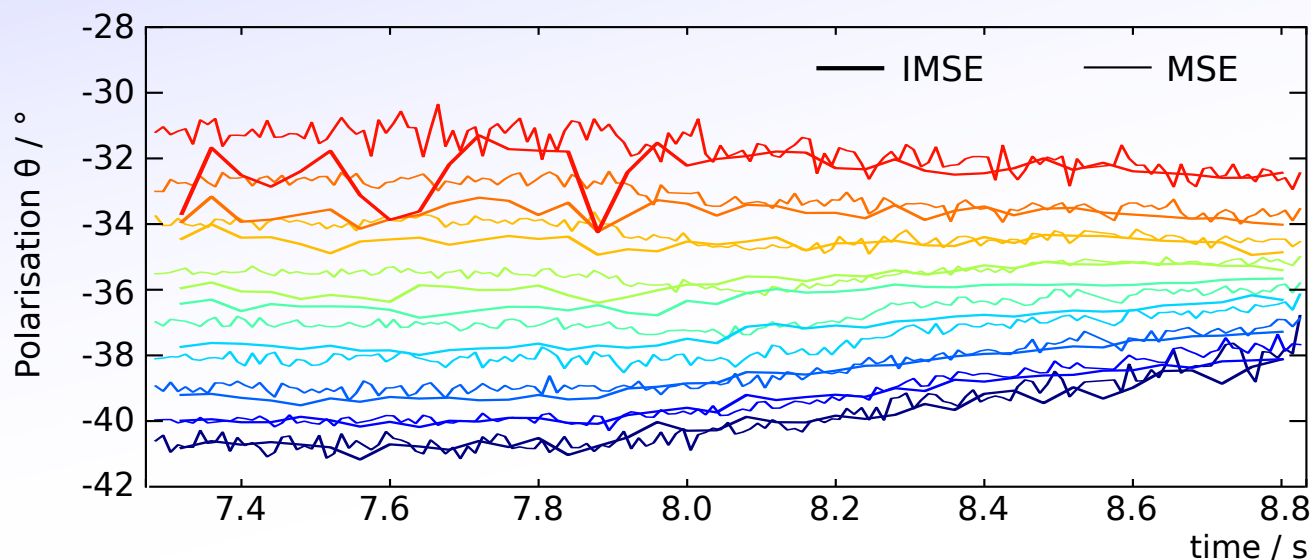
The imaging nature of the system allows easy position calibration by identifying known features in a background image and calculating the intersection with the neutral beam:





# Direct MSE - IMSE comparison

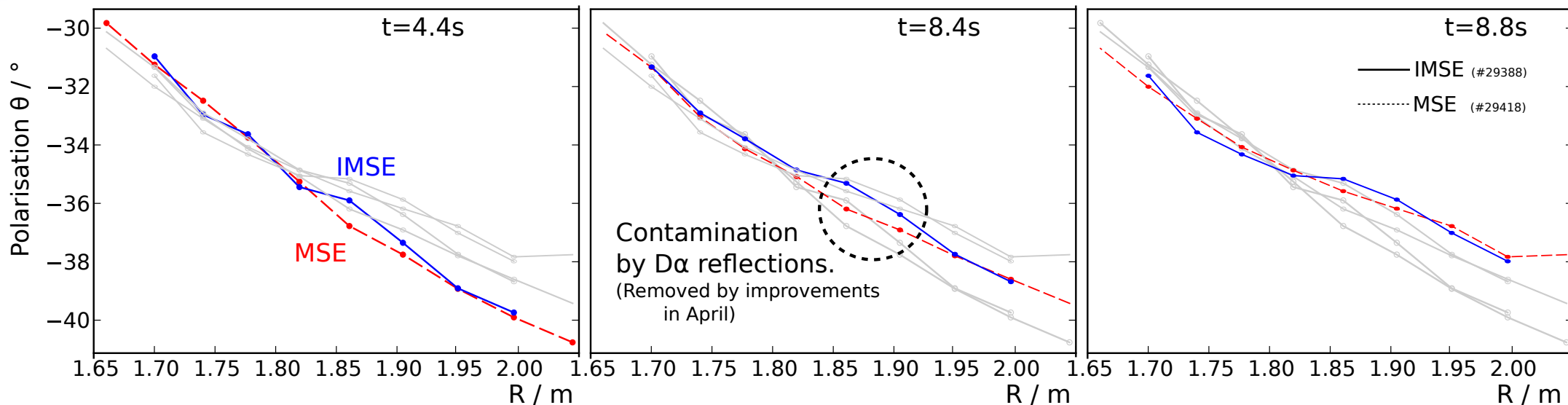
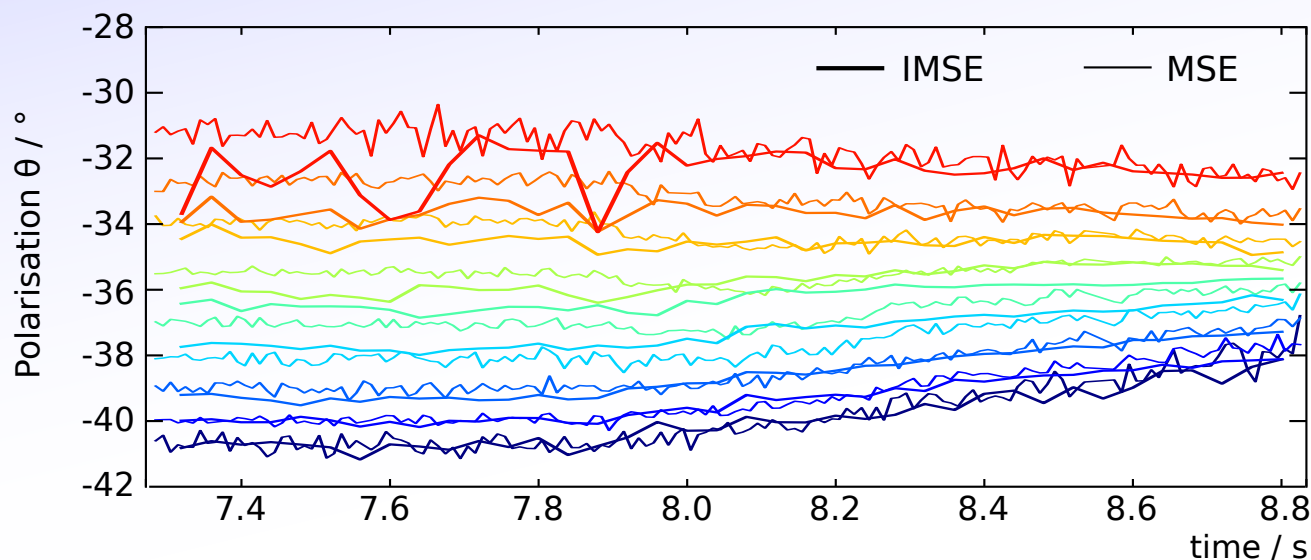
To compare the IMSE and MSE systems directly, the same plasma shot was run with the MSE system in the following week. Except for a  $1.1^\circ$  offset, the agreement is good:





# Direct MSE - IMSE comparison

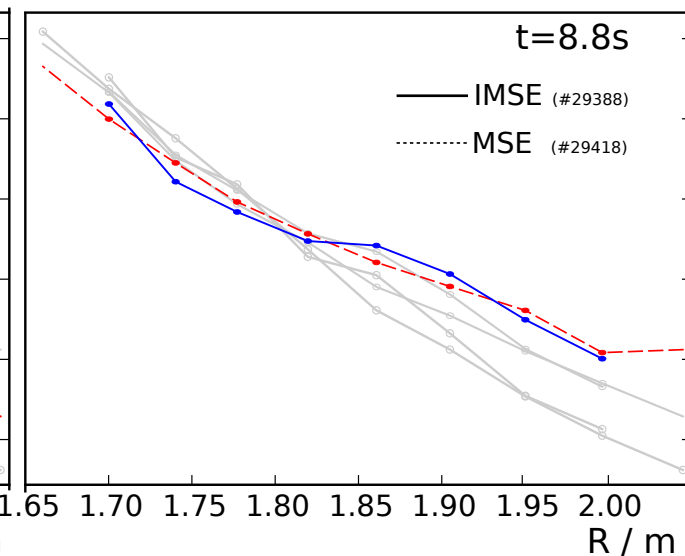
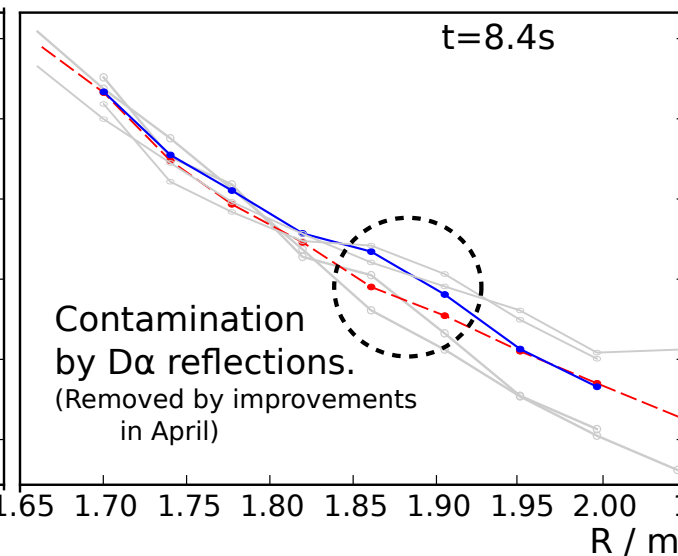
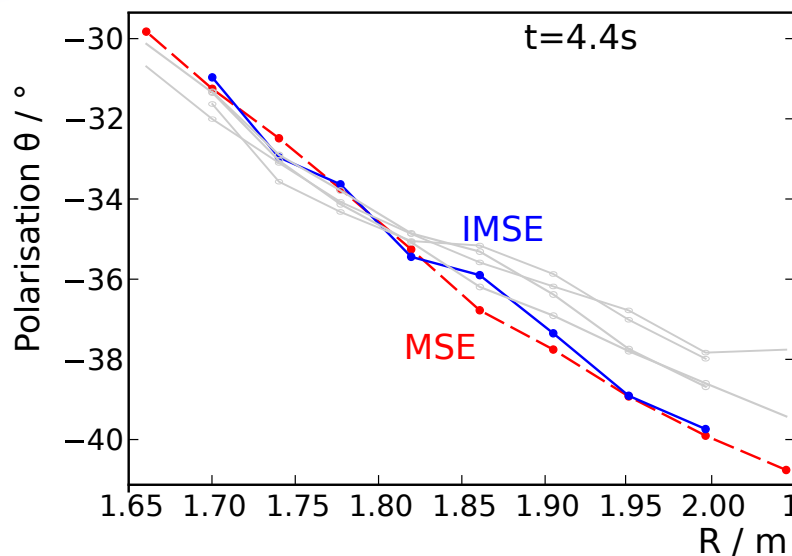
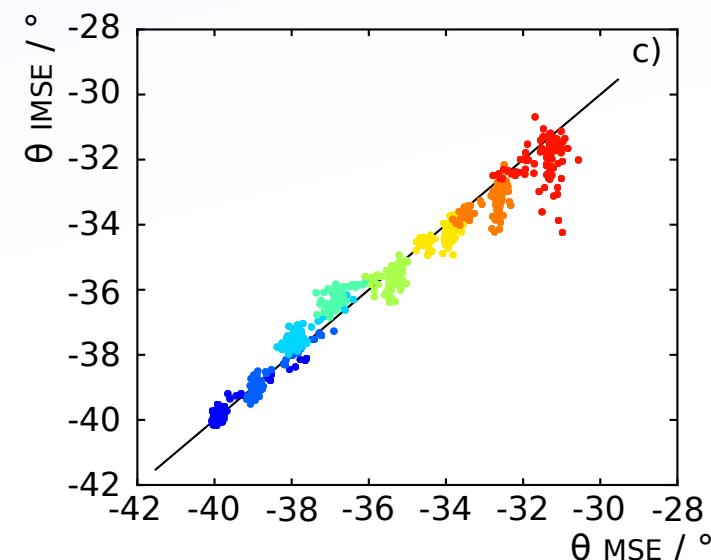
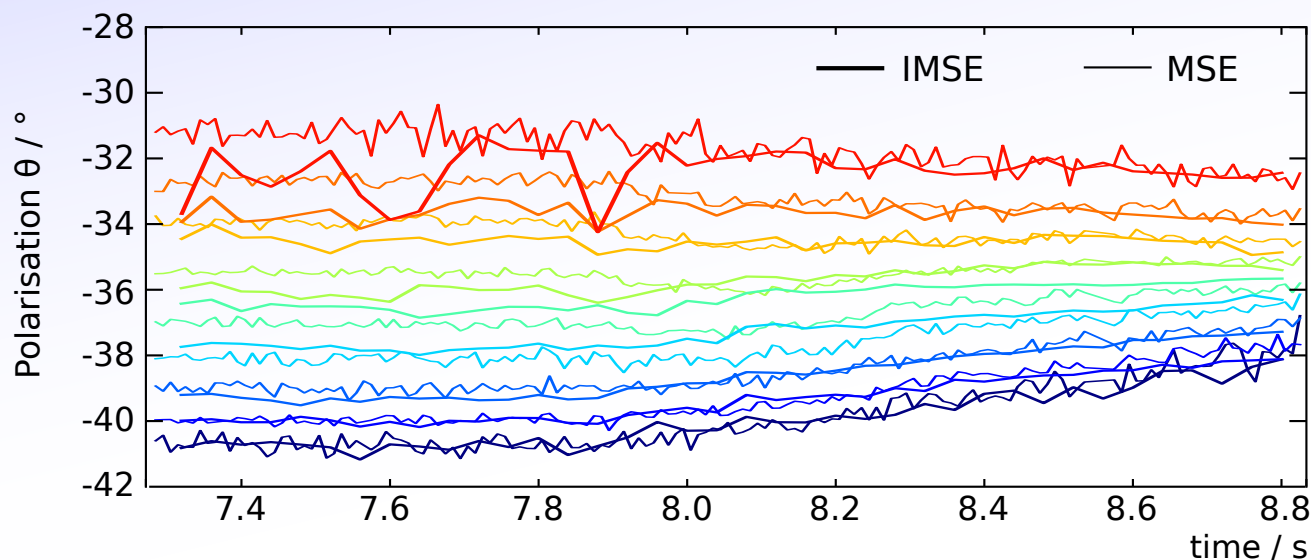
To compare the IMSE and MSE systems directly, the same plasma shot was run with the MSE system in the following week. Except for a 1.1° offset, the agreement is good:





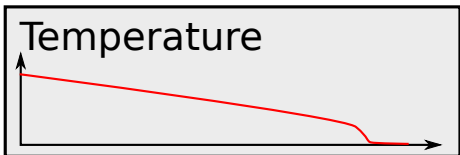
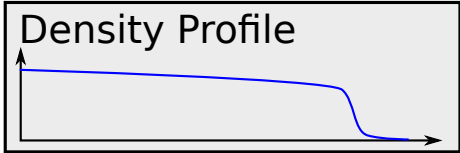
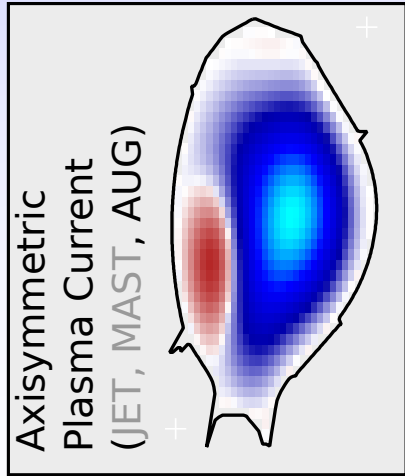
# Direct MSE - IMSE comparison

To compare the IMSE and MSE systems directly, the same plasma shot was run with the MSE system in the following week. Except for a 1.1° offset, the agreement is good:



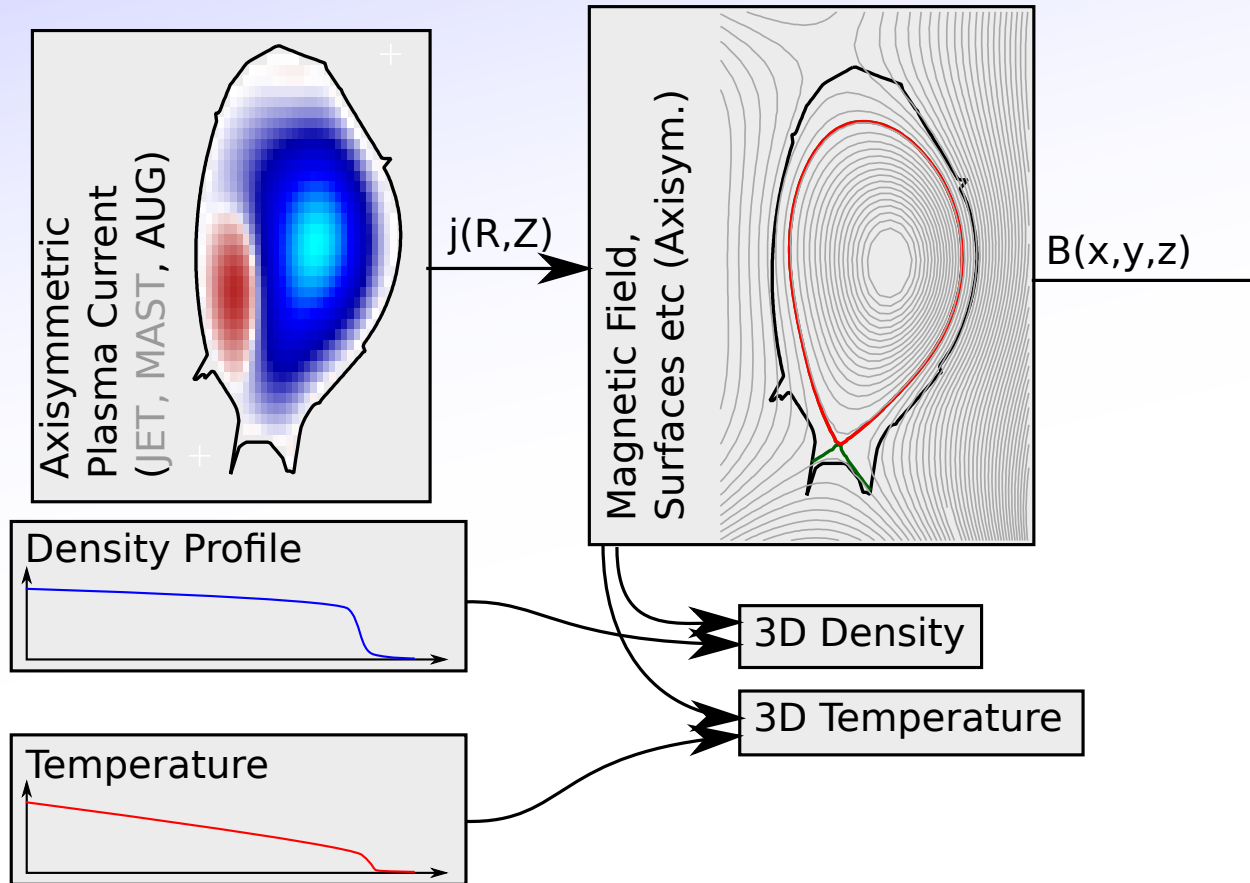
# Forward Model

Developed several components for the Bayesian / forward modelling framework (Minerva).



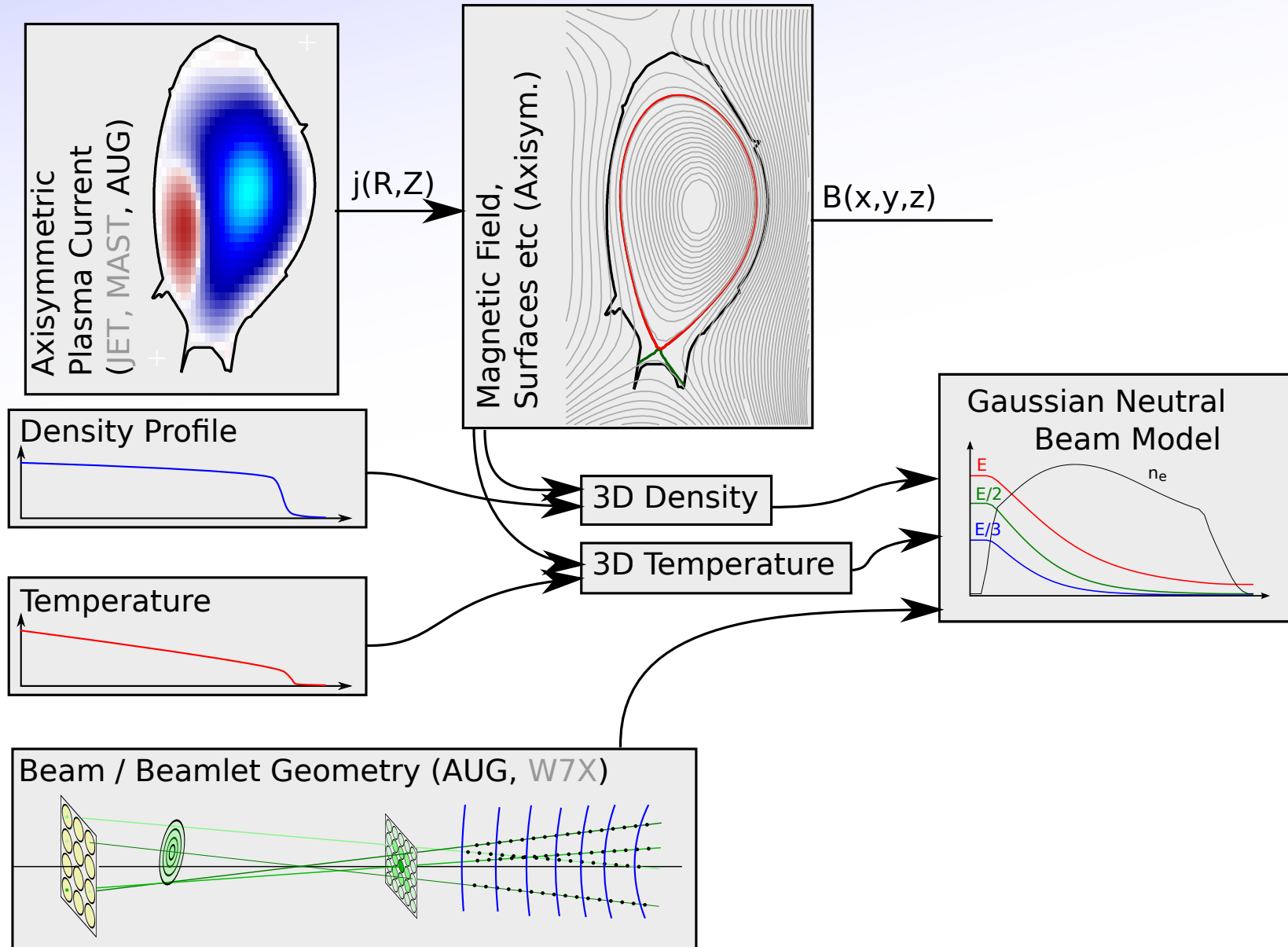
# Forward Model

Developed several components for the Bayesian / forward modelling framework (Minerva).



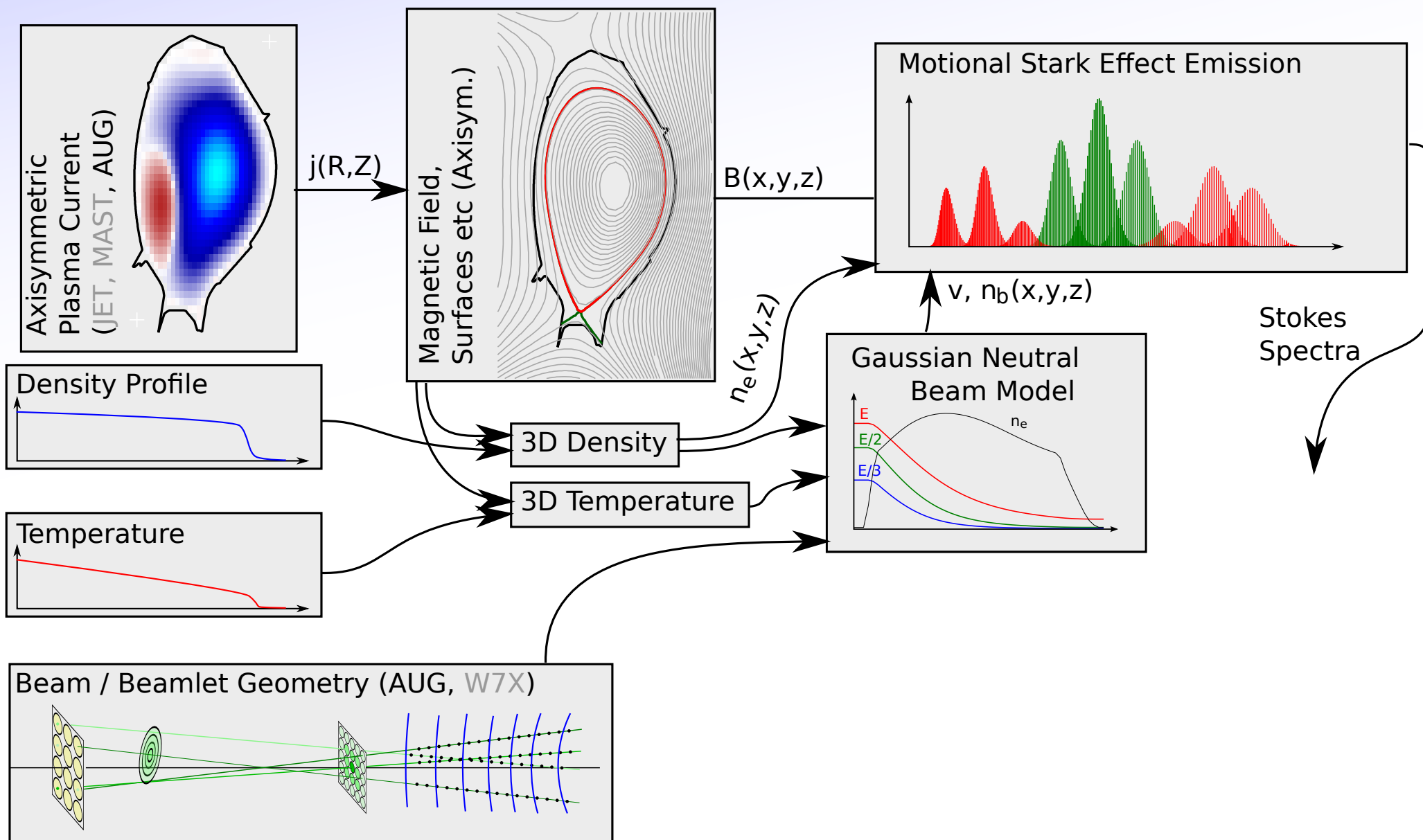
# Forward Model

Developed several components for the Bayesian / forward modelling framework (Minerva).



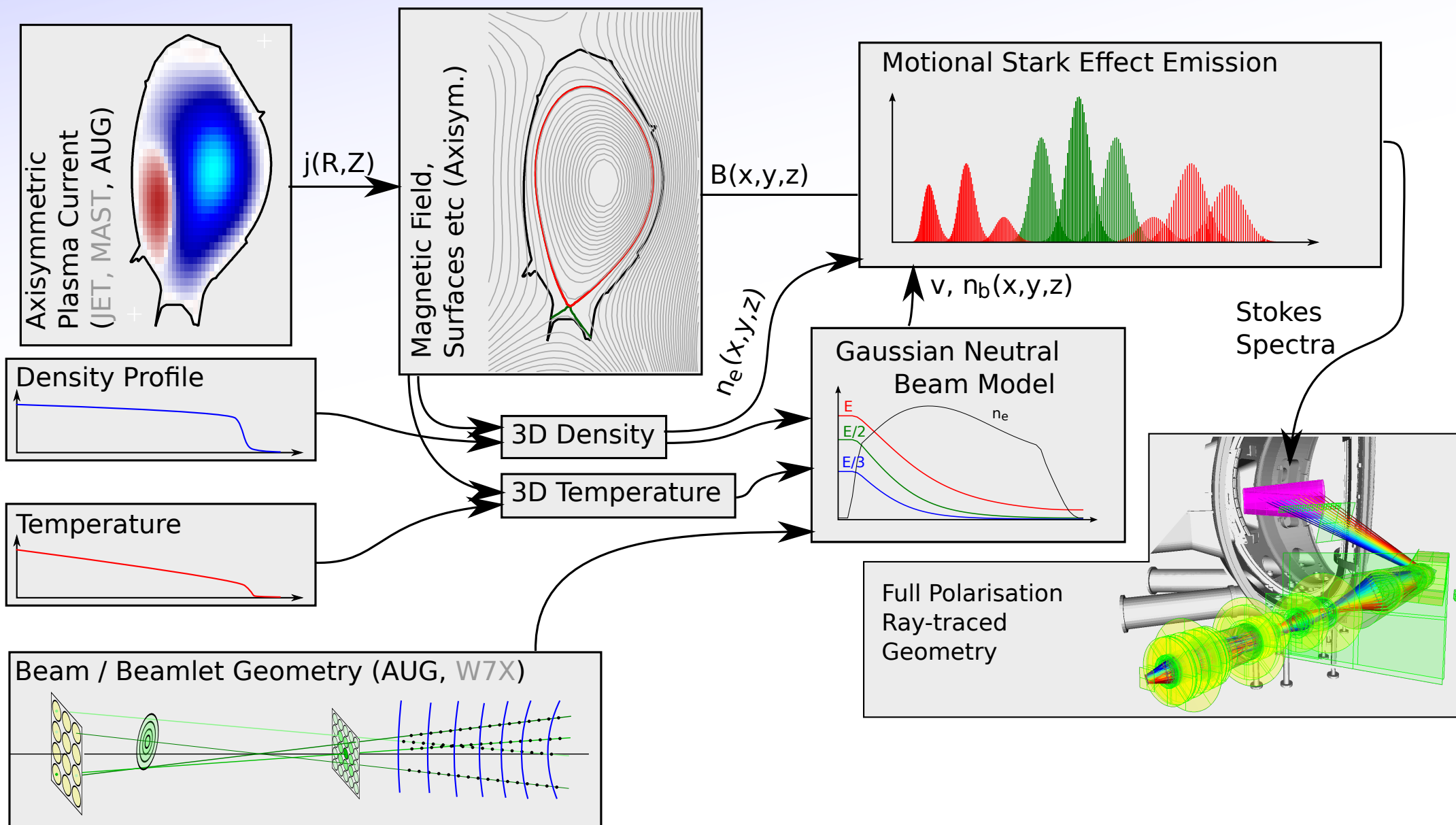
# Forward Model

Developed several components for the Bayesian / forward modelling framework (Minerva).



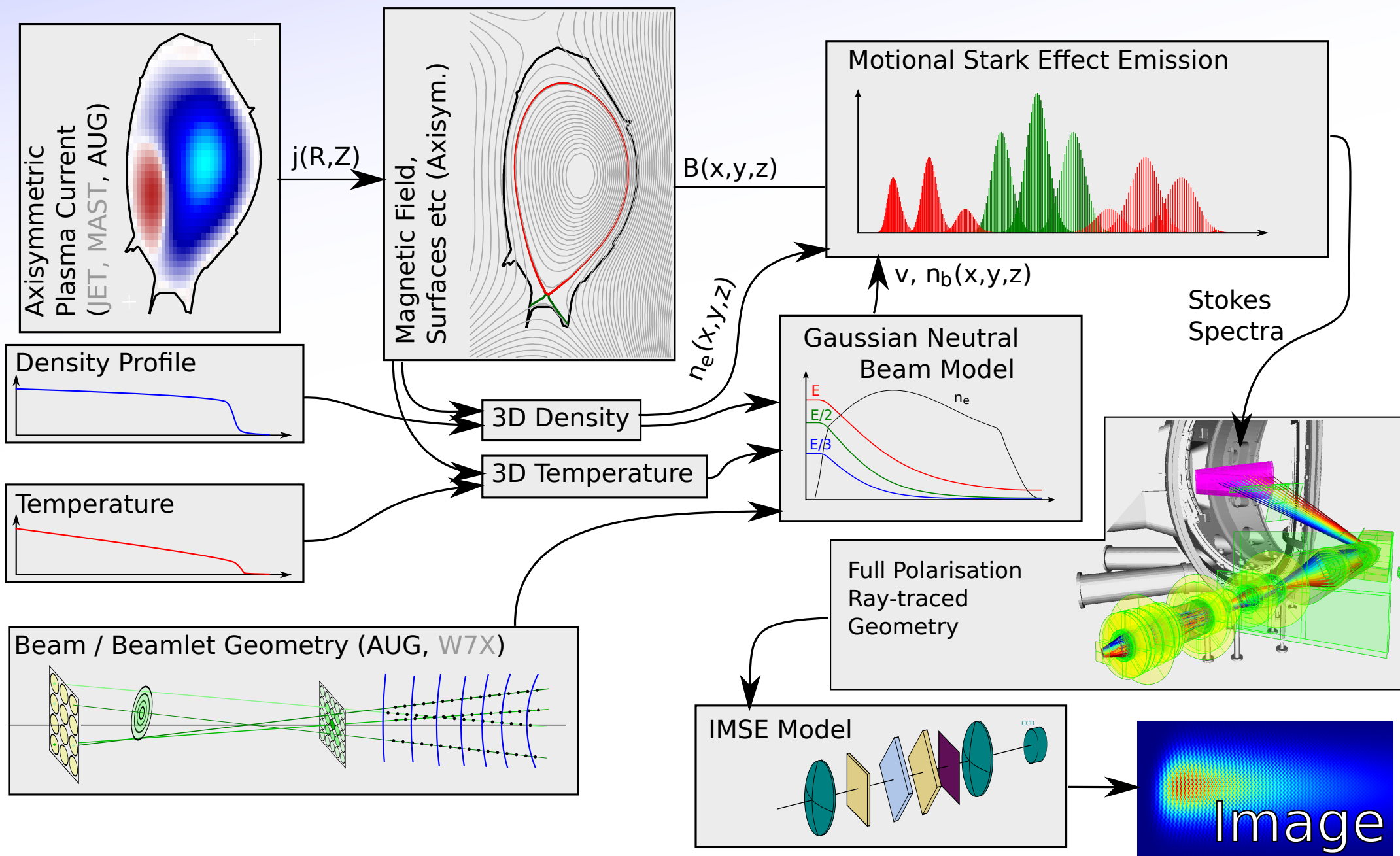
# Forward Model

Developed several components for the Bayesian / forward modelling framework (Minerva).



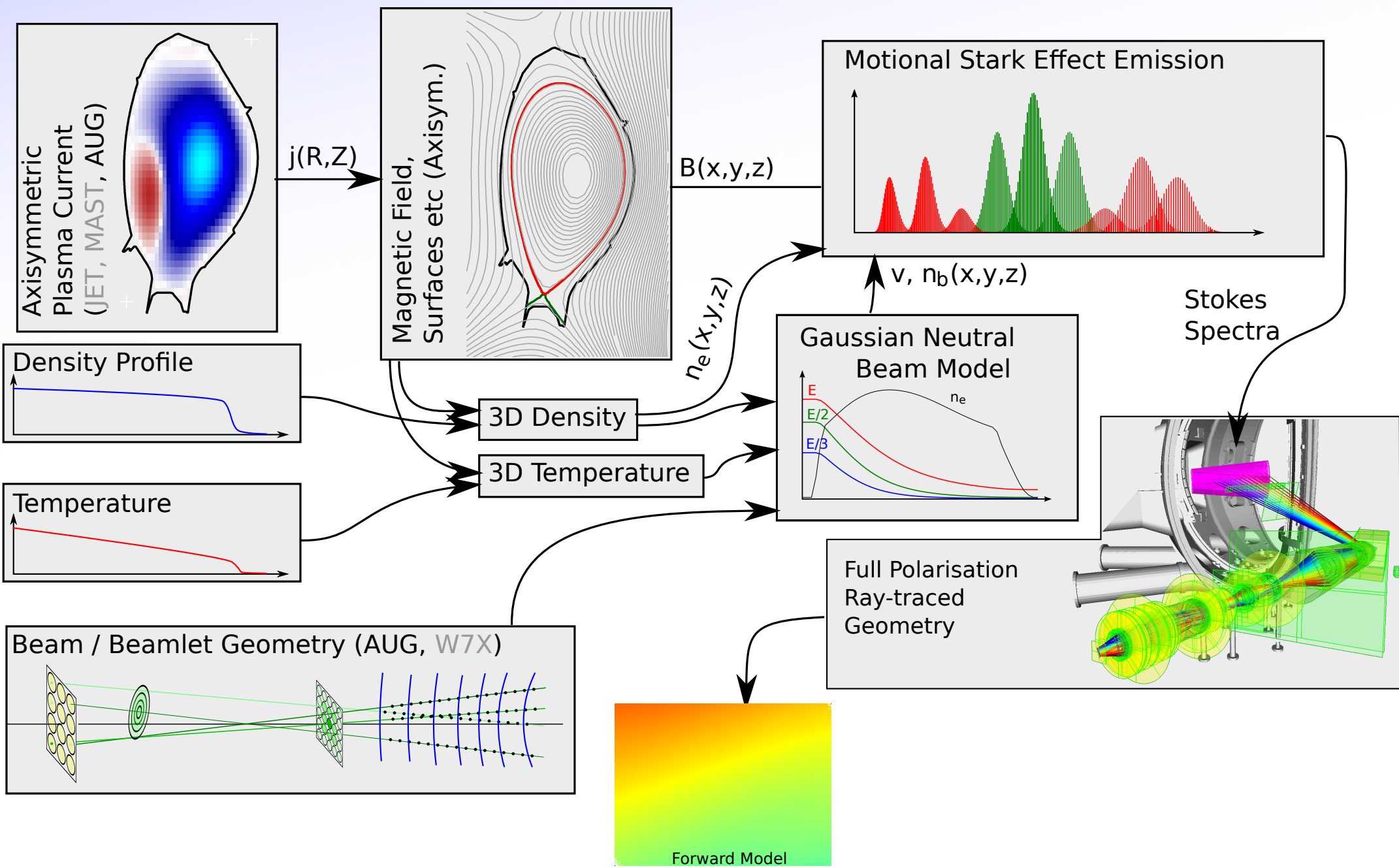
# Forward Model

Developed several components for the Bayesian / forward modelling framework (Minerva).



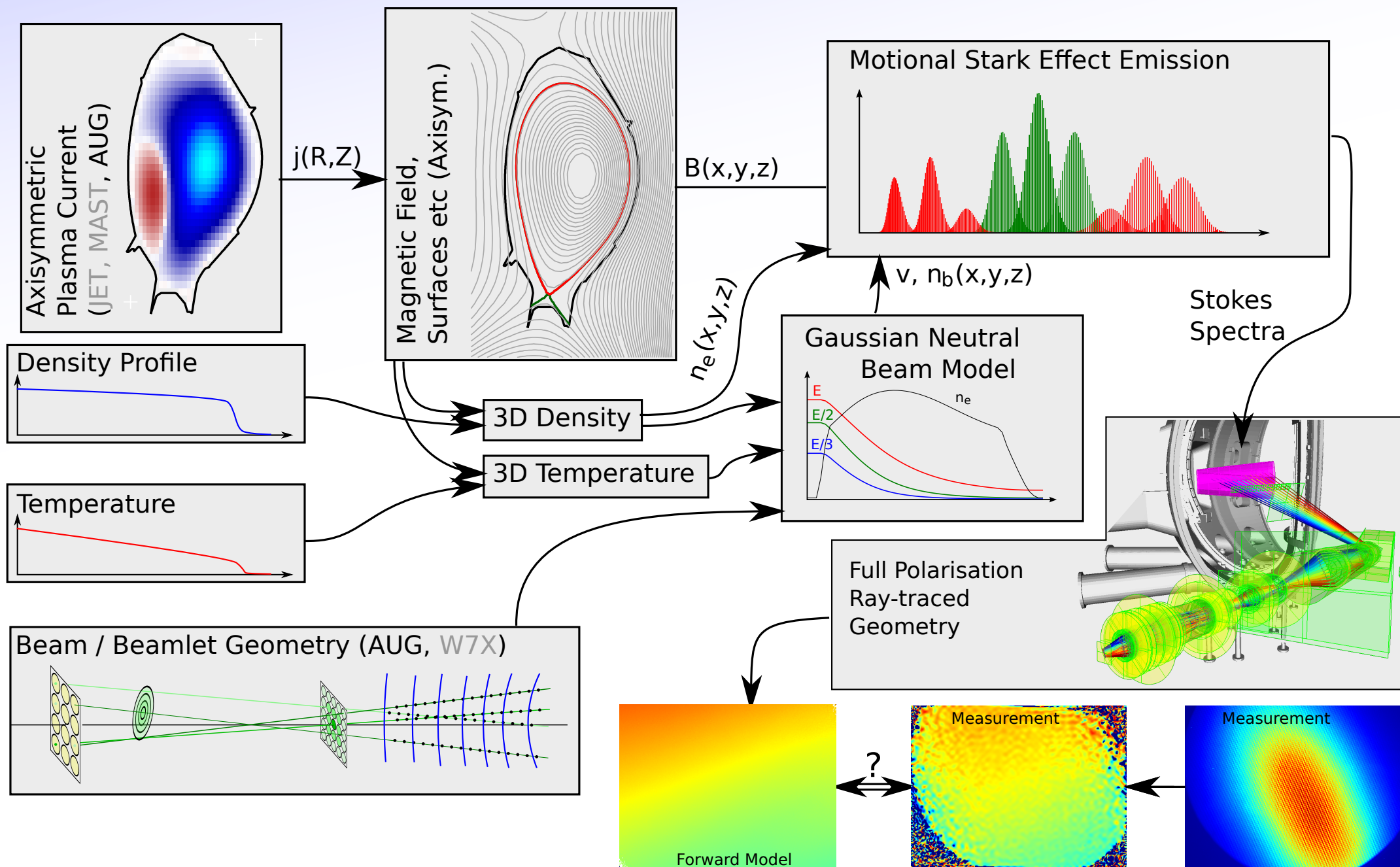
# Forward Model

Developed several components for the Bayesian / forward modelling framework (Minerva).

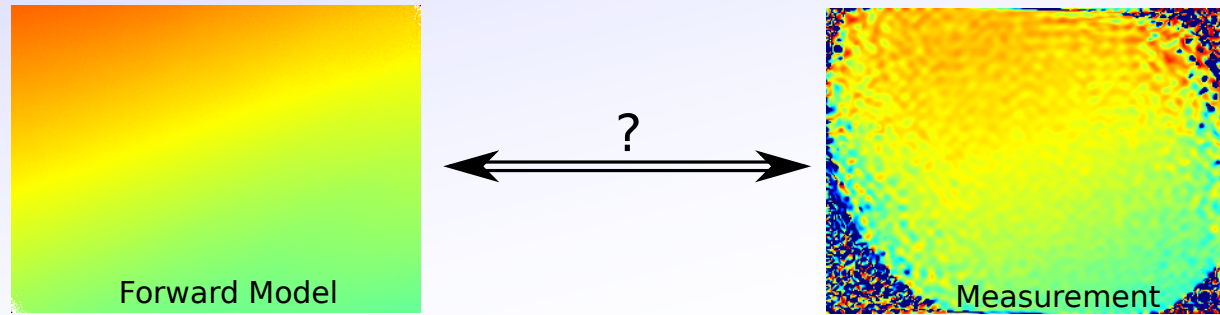


# Forward Model

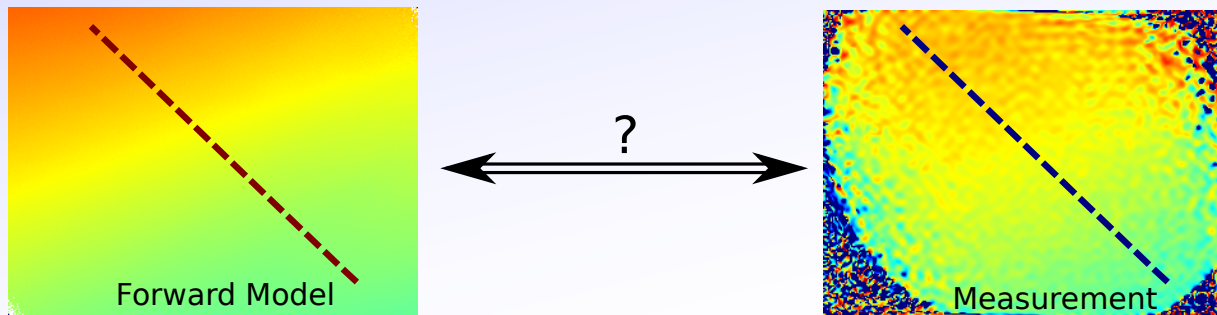
Developed several components for the Bayesian / forward modelling framework (Minerva).



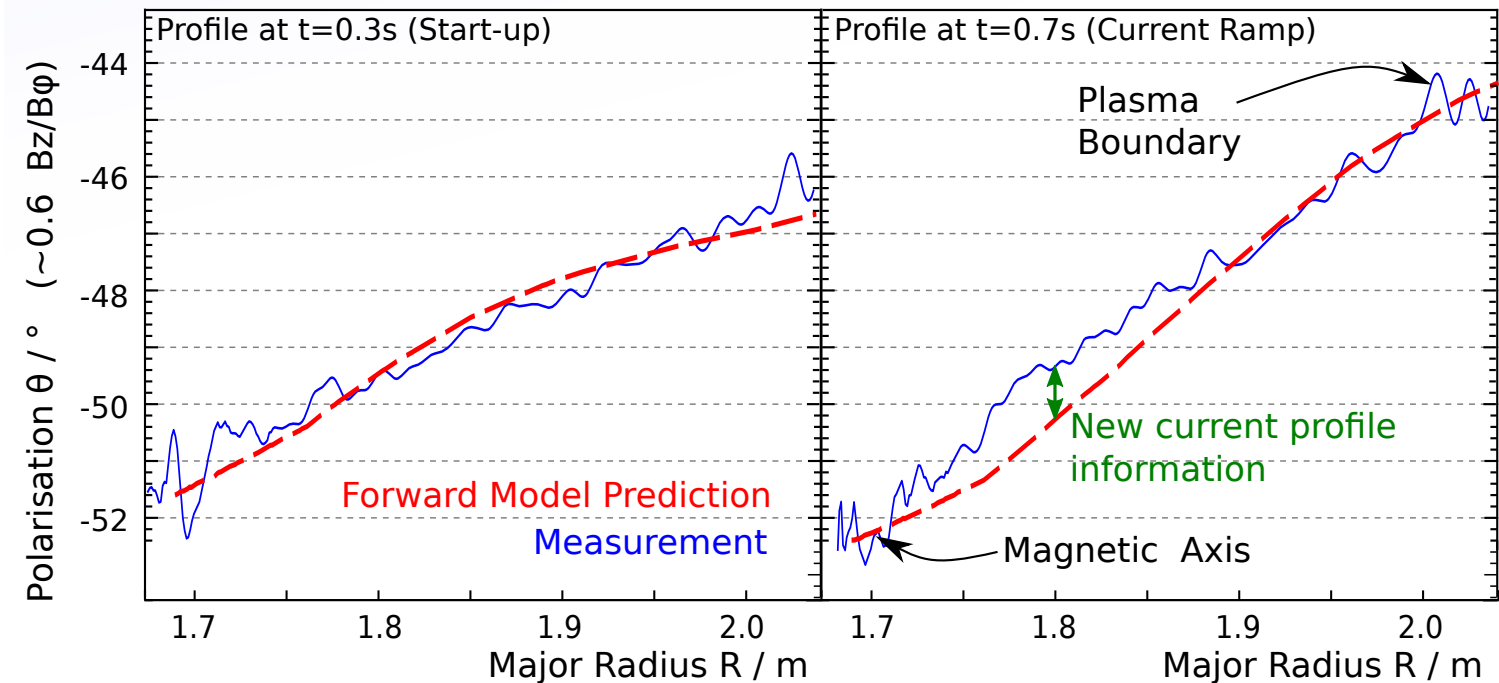
# Comparison with Forward Model (1D)



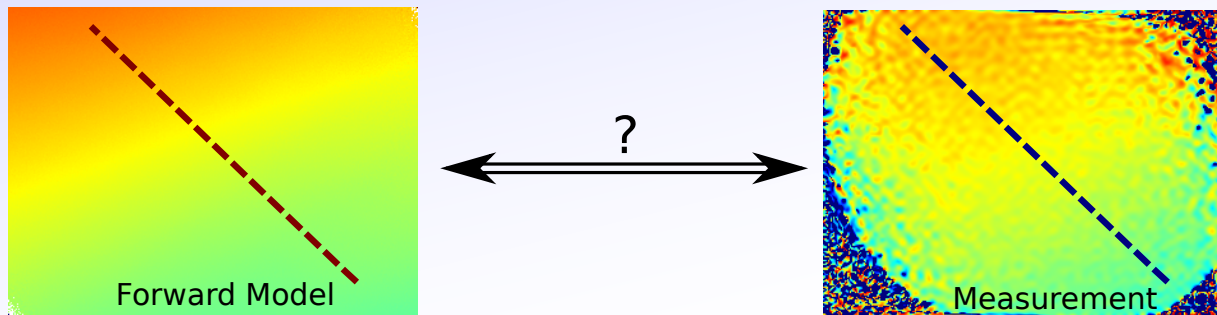
# Comparison with Forward Model (1D)



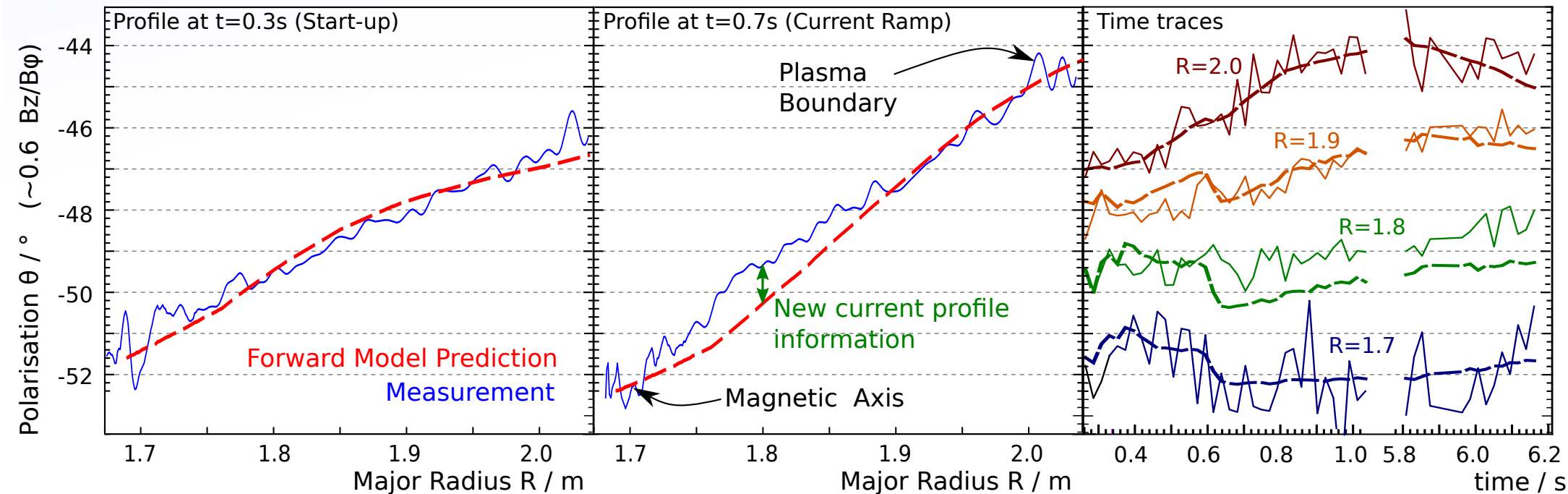
Compared directly with the measurement, there is only a  $0.7^\circ$  offset. Once subtracted, it agrees during current ramp with the regions where the equilibrium/CT is expected to correctly predict the pitch angle:



# Comparison with Forward Model (1D)



Compared directly with the measurement, there is only a  $0.7^\circ$  offset. Once subtracted, it agrees during current ramp with the regions where the equilibrium/CT is expected to correctly predict the pitch angle:

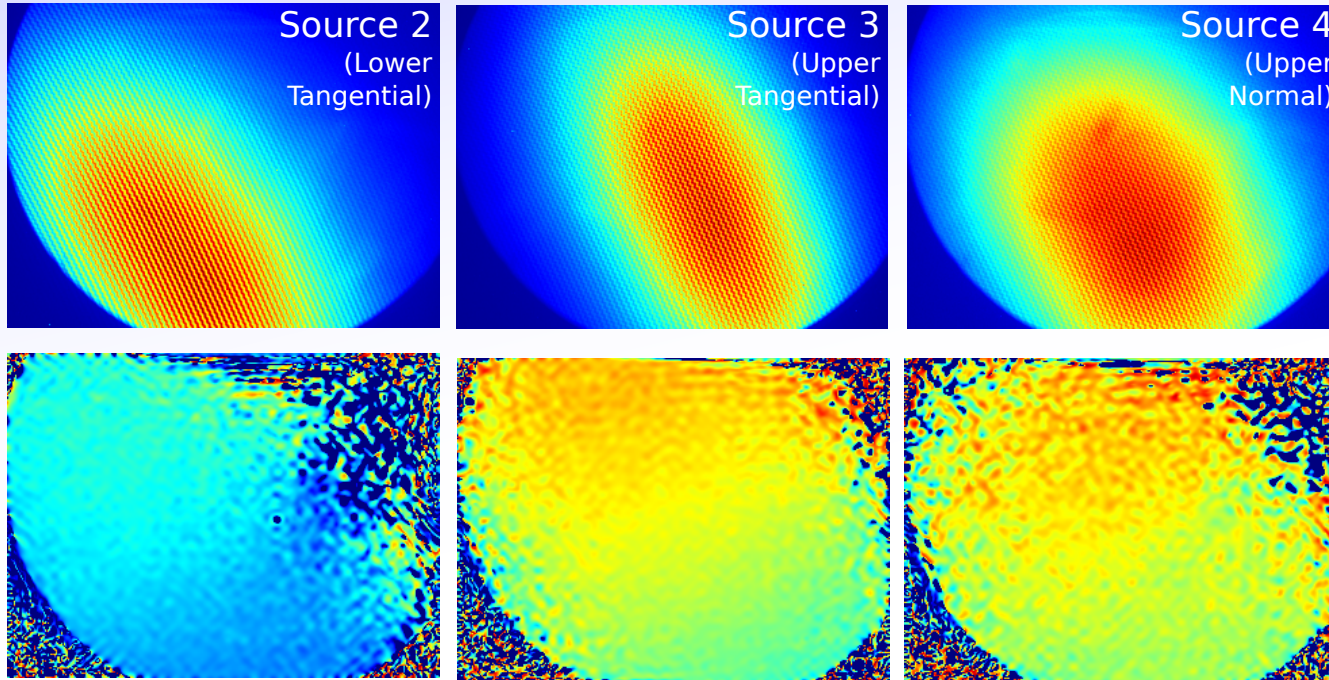


At present, the diagnostic has **no angle calibration**. The forward model is based entirely on the CAD and optics models and the measurement is unprocessed.

The disagreement at mid-radius is useful information that will be used to constrain the current profile.

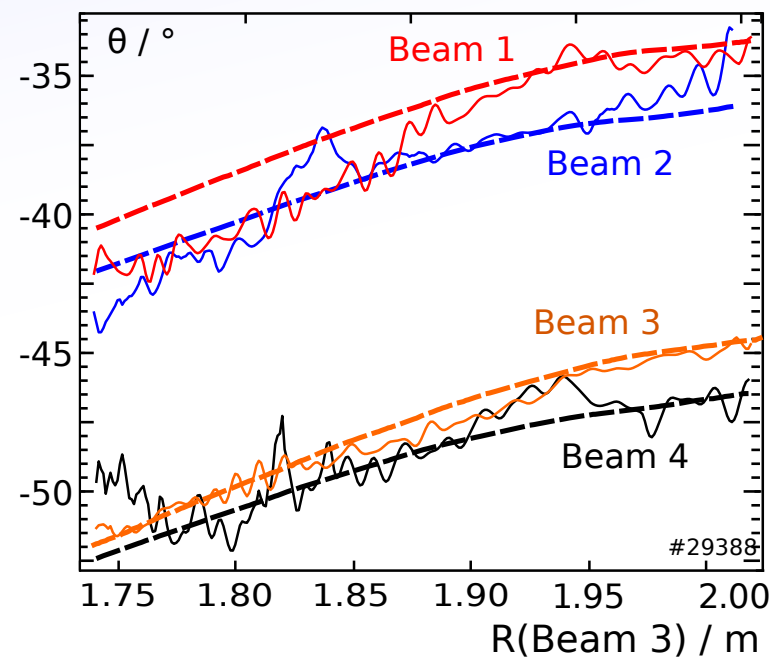
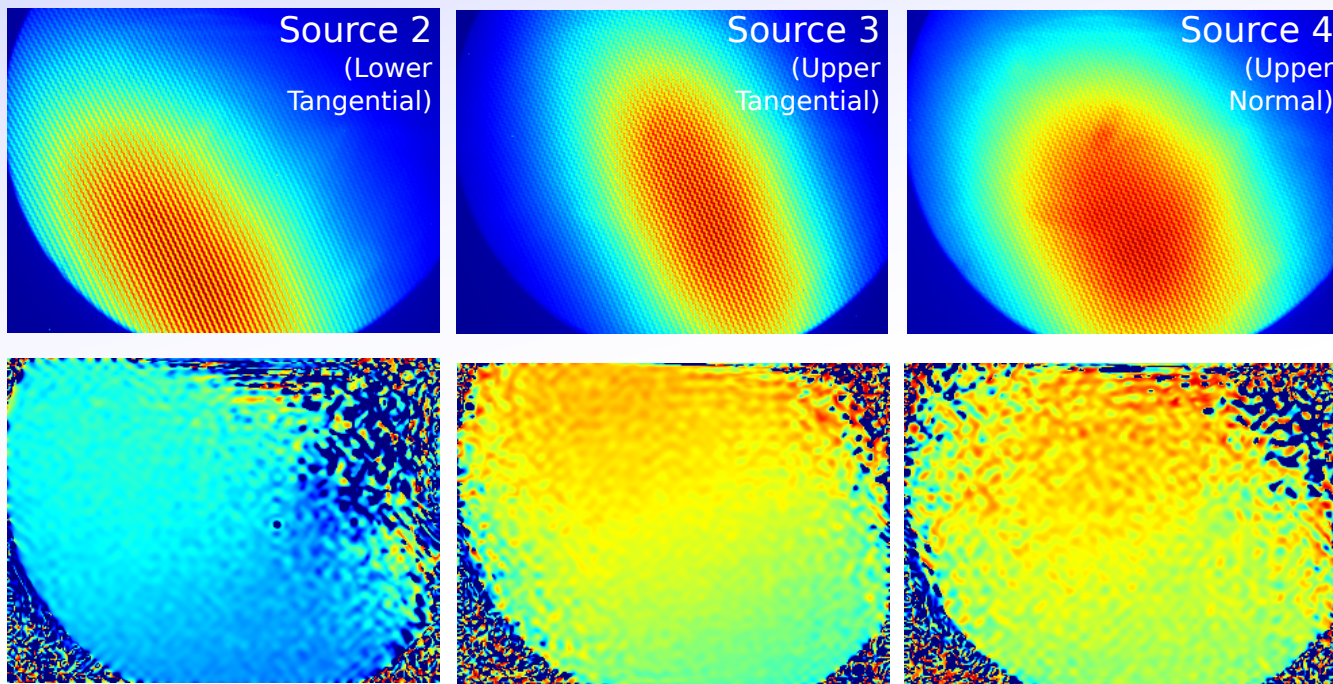
# Beam Configuration Insensitivity

IMSE is insensitive to the spectrum so works on all 4 beam sources with both Deuterium and Hydrogen fuel:



# Beam Configuration Insensitivity

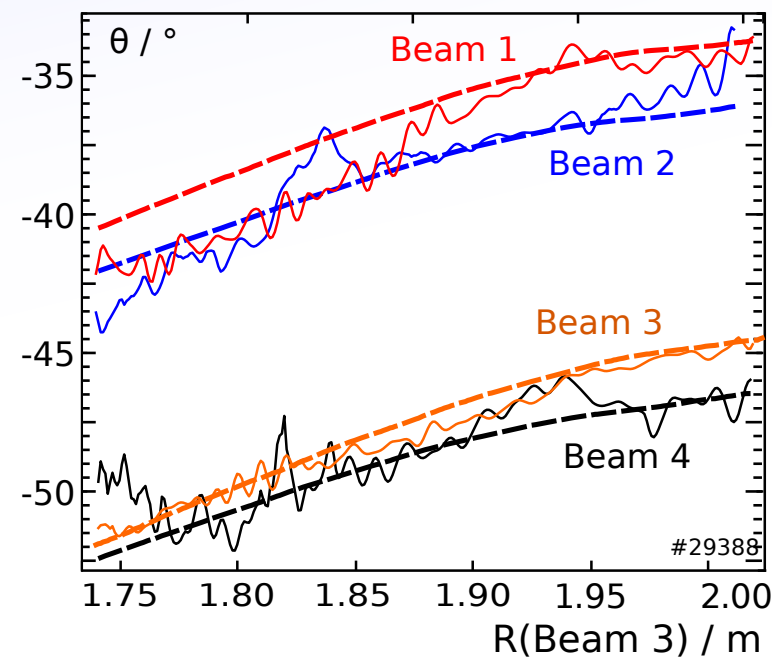
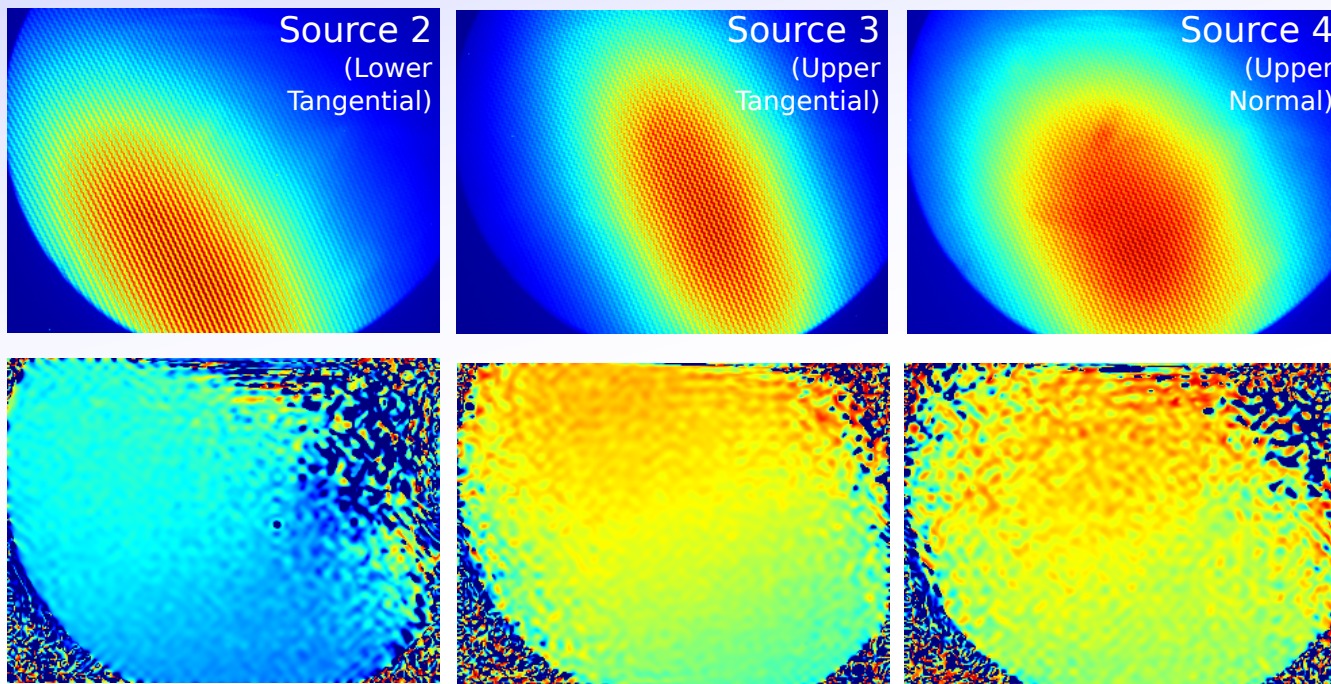
IMSE is insensitive to the spectrum so works on all 4 beam sources with both Deuterium and Hydrogen fuel:



$\theta_3 - \theta_1$  is a fixed geometry value, so the agreement confirms the diagnostic linearity and beam geometry.  
 $\theta_3 - \theta_4$  (or  $\theta_2 - \theta_1$ ) relate directly to  $B_z/B_\phi$  and are unaffected by fixed offset errors.

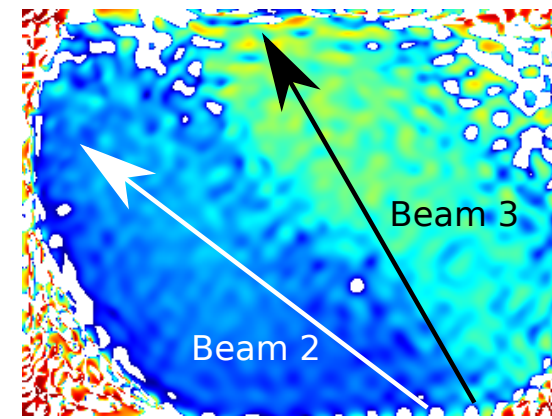
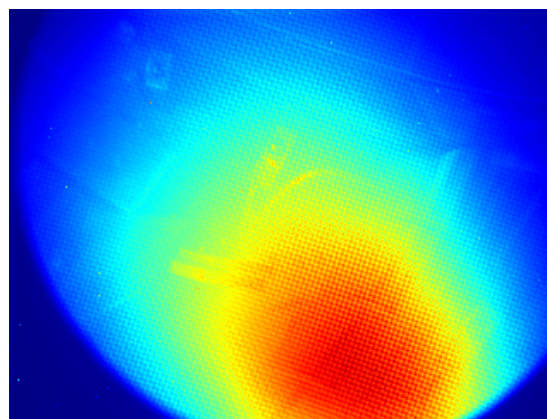
# Beam Configuration Insensitivity

IMSE is insensitive to the spectrum so works on all 4 beam sources with both Deuterium and Hydrogen fuel:

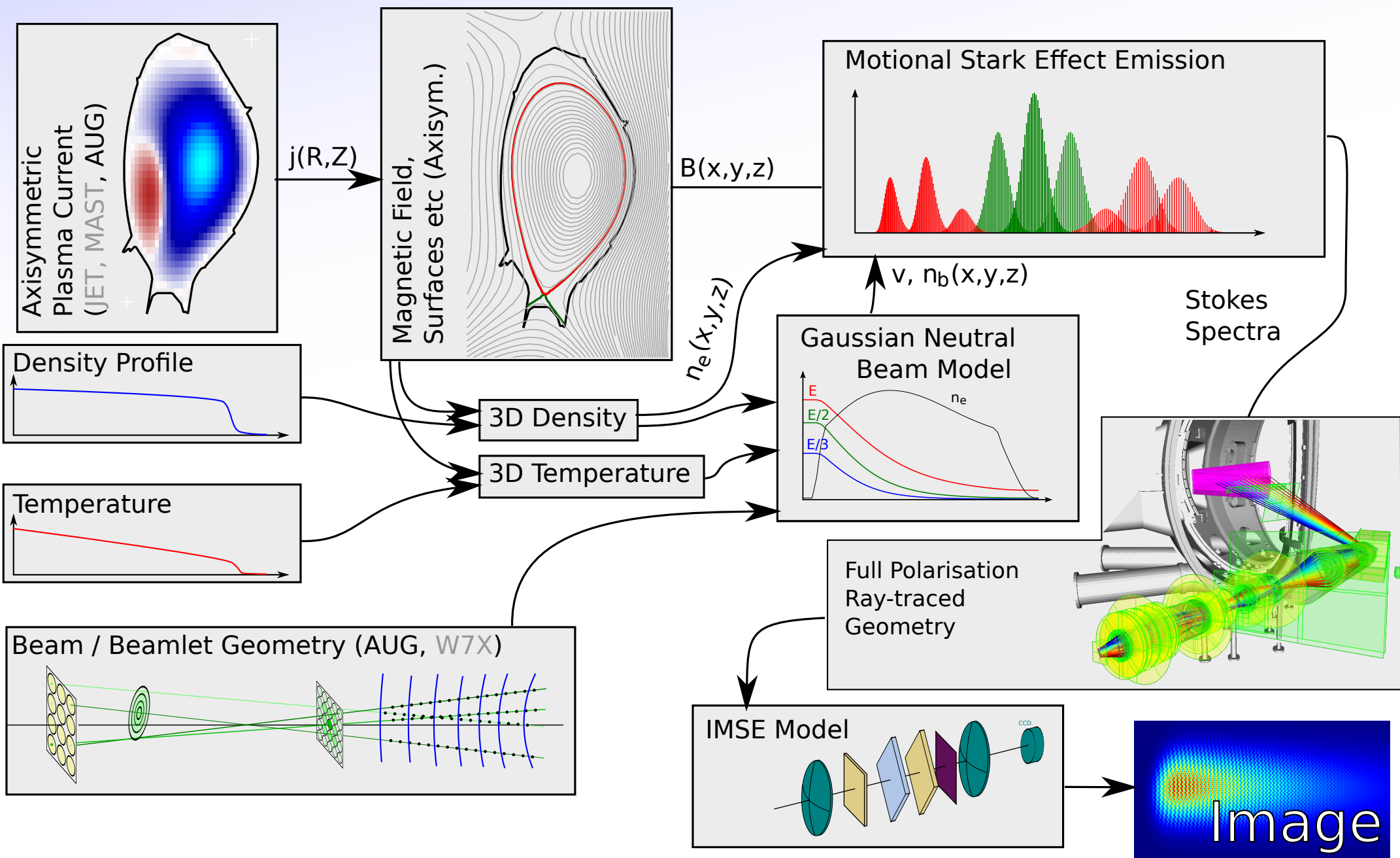


$\theta_3 - \theta_1$  is a fixed geometry value, so the agreement confirms the diagnostic linearity and beam geometry.  
 $\theta_3 - \theta_4$  (or  $\theta_2 - \theta_1$ ) relate directly to  $B_z/B_\phi$  and are unaffected by fixed offset errors.

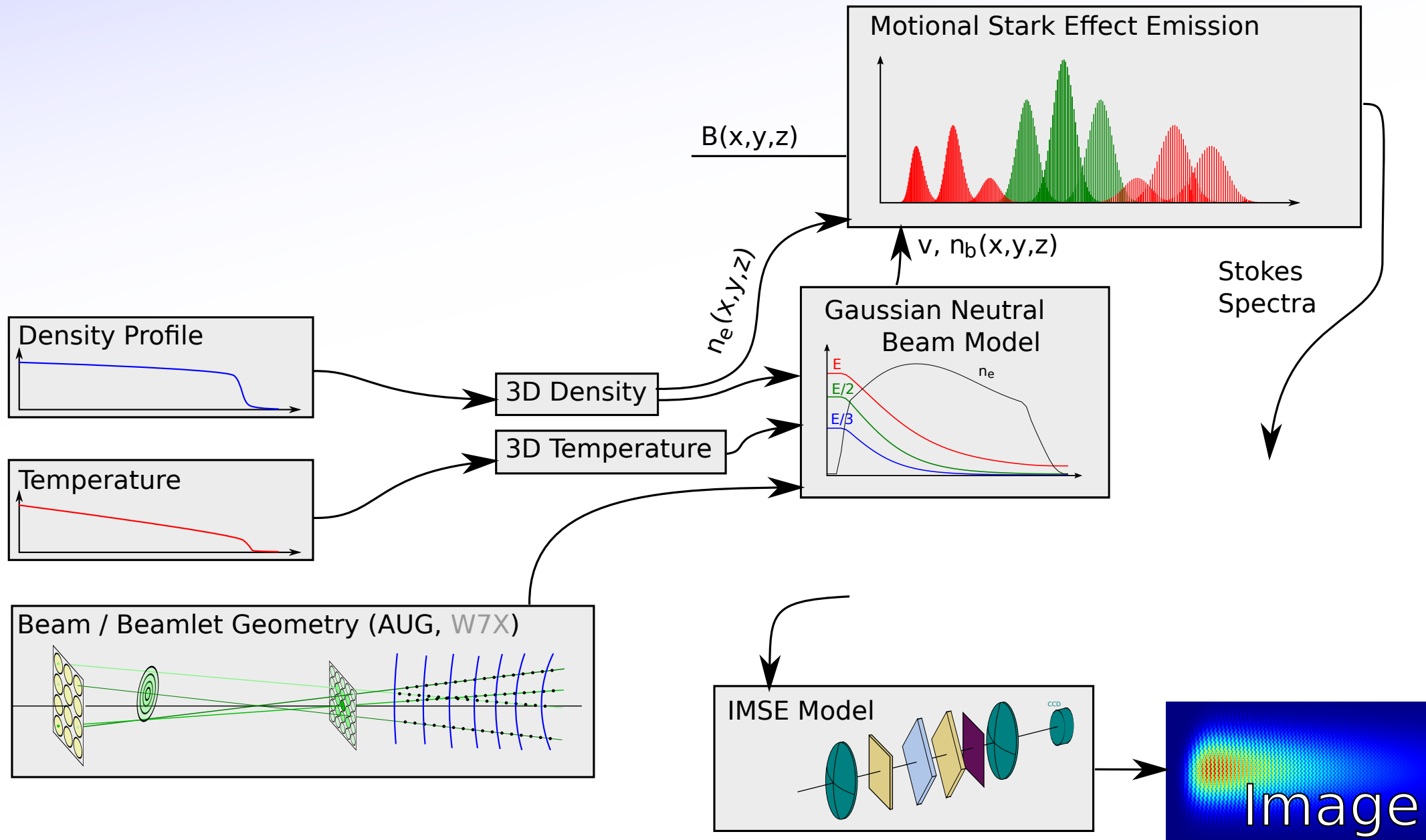
In principle, it is also possible to use data when multiple beams are on. The data is a complex average but can be analysed with the forward model if the beam geometry model is accurate.



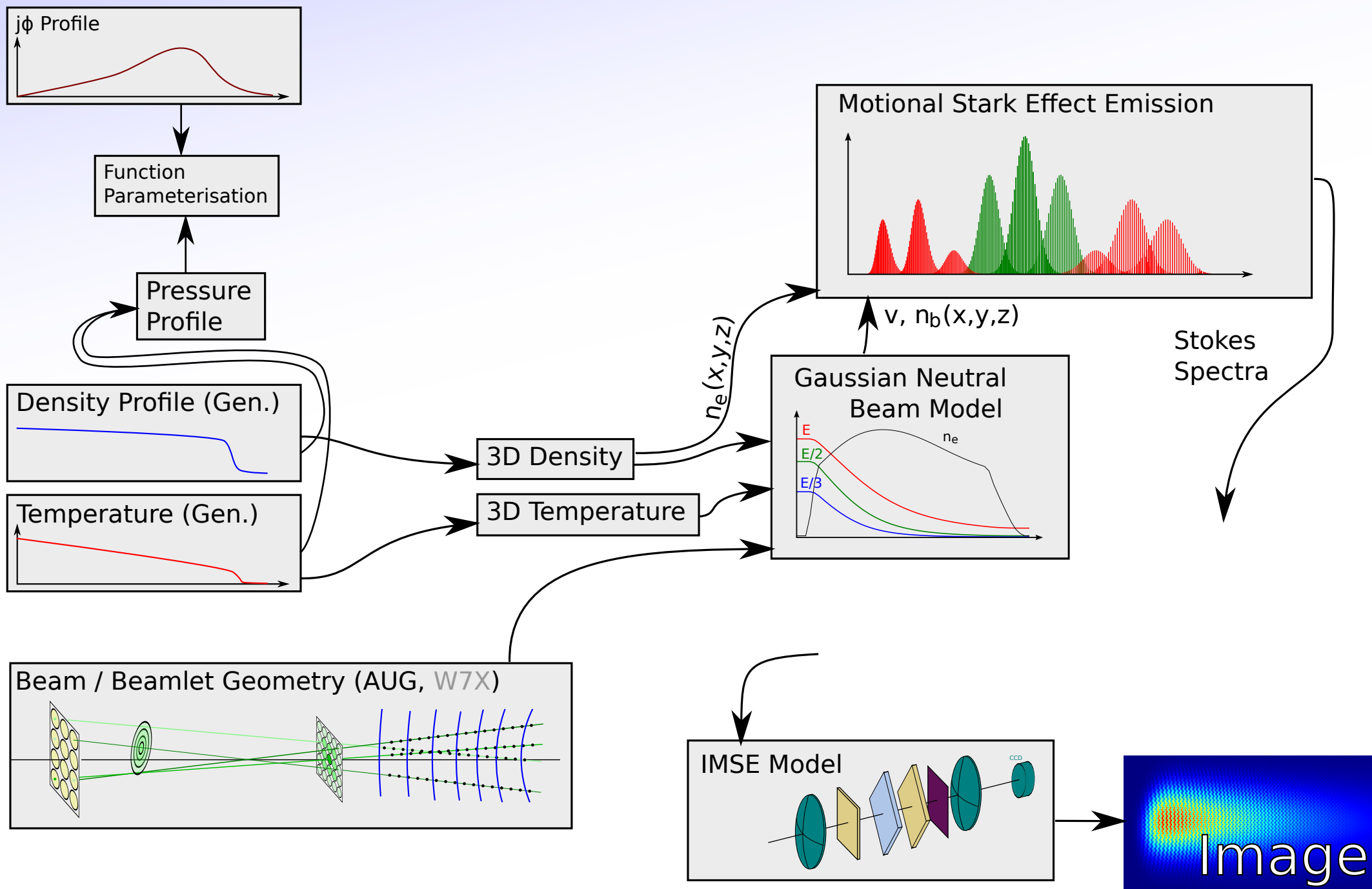
# Forward Model (AUG)



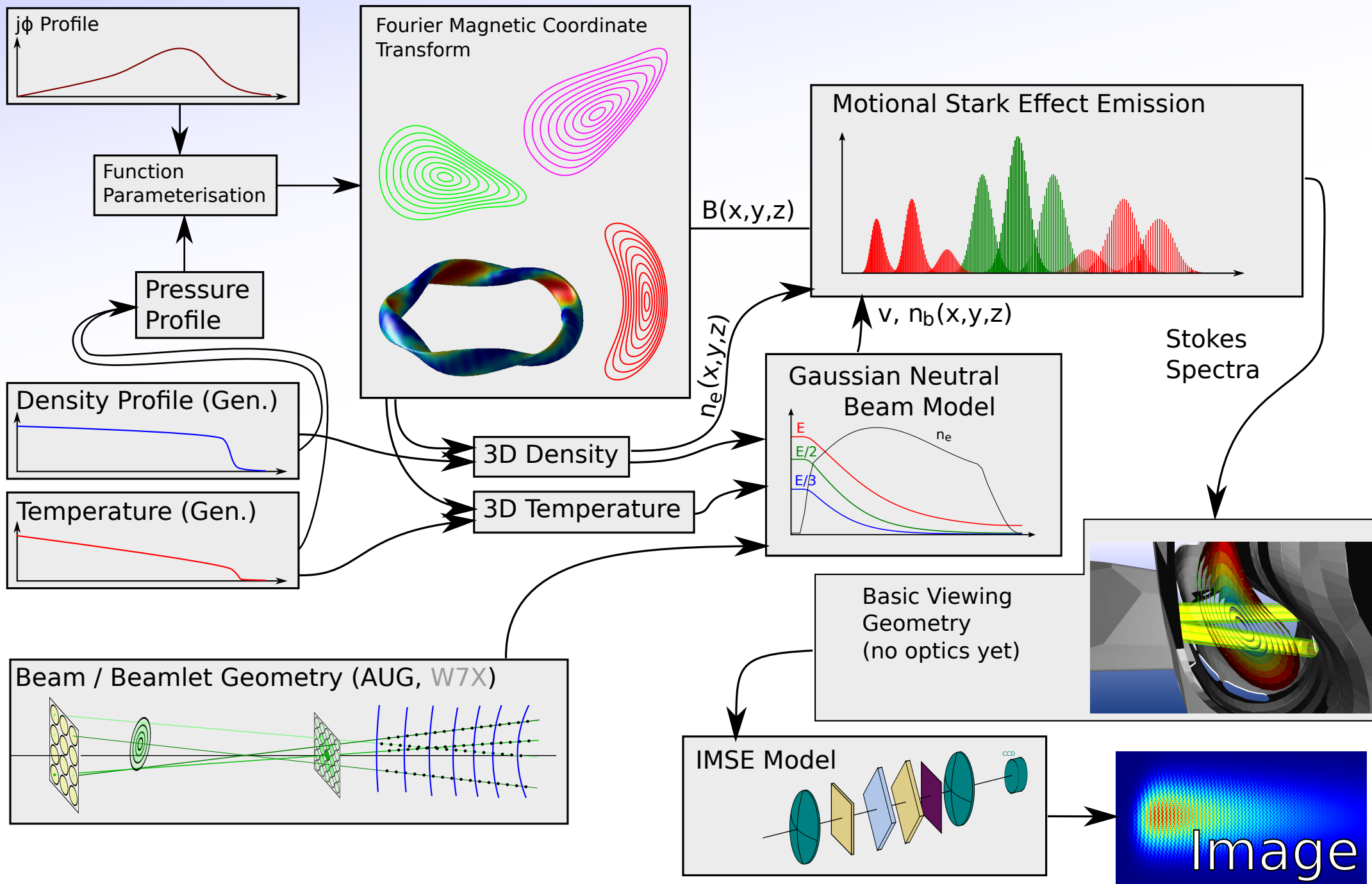
# Forward Model (W7X)



# Forward Model (W7X)



# Forward Model (W7X)

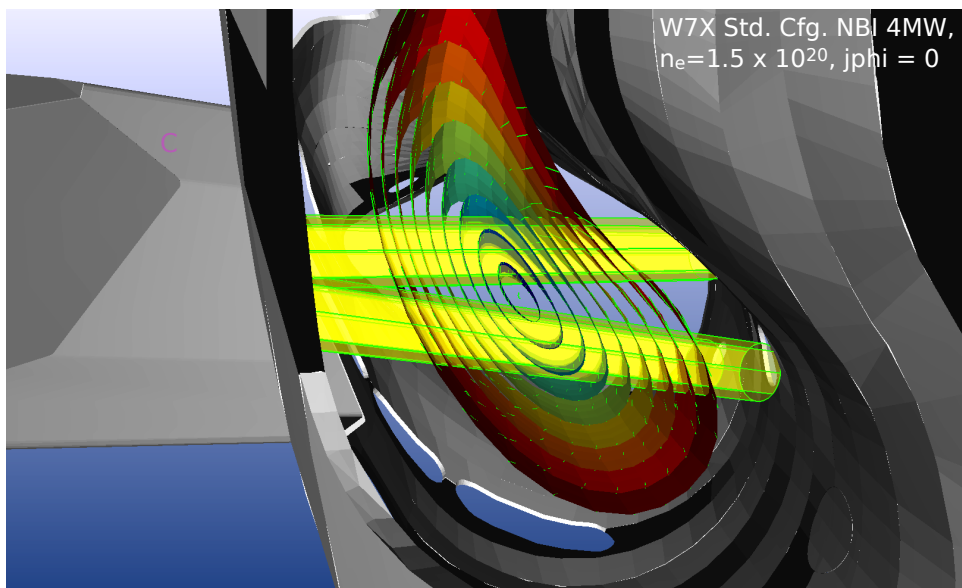
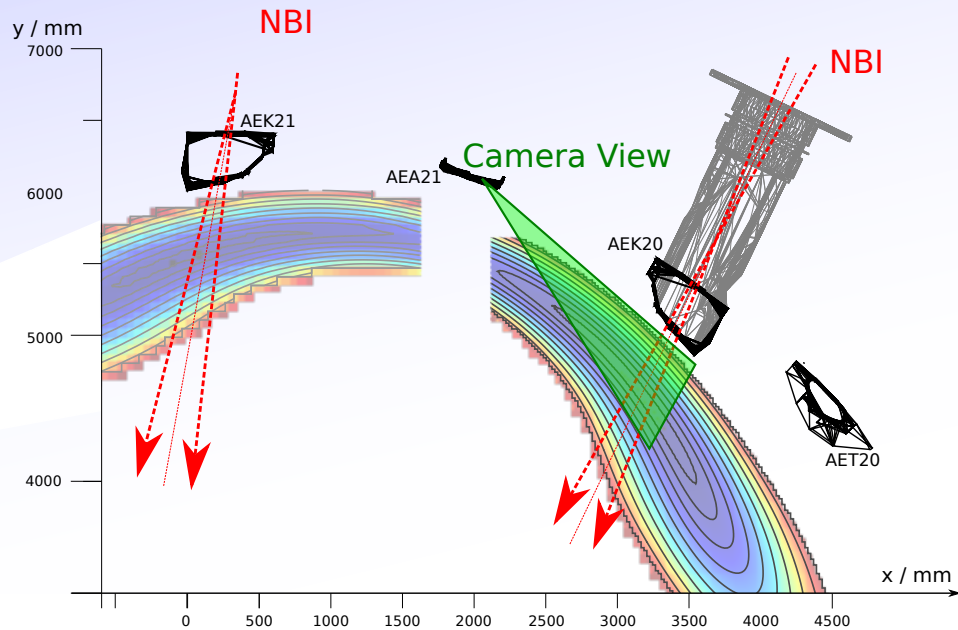


# Geometry (W7X)



Image intensity.

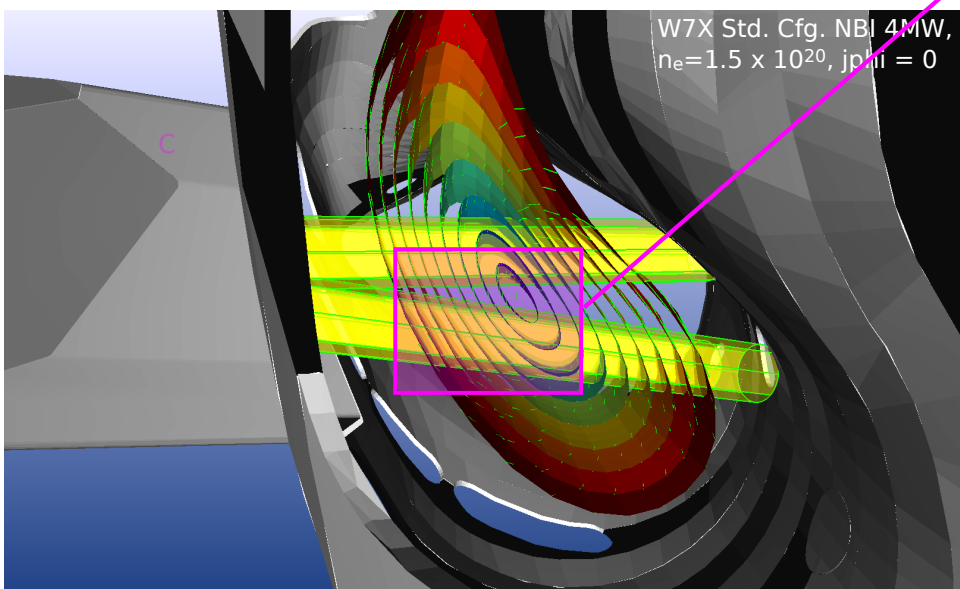
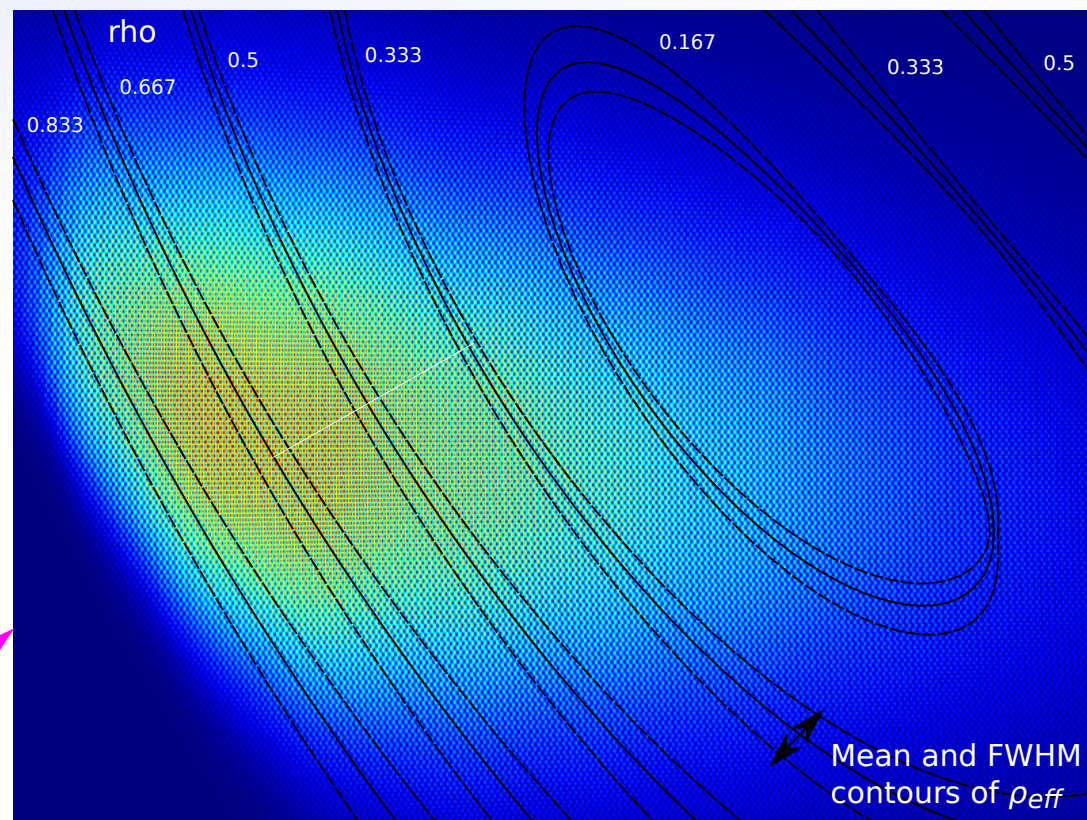
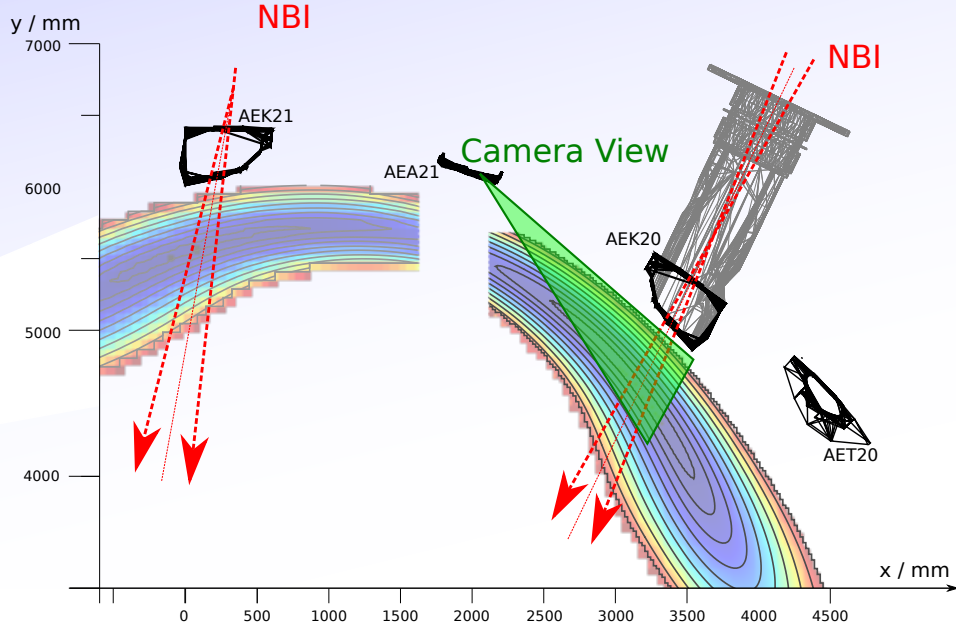
A port in between the two NBI boxes is available for the CXRS and MSE systems which gives good spatial resolution.



# Geometry (W7X)



A port in between the two NBI boxes is available for the CXRS and MSE systems which gives good spatial resolution.

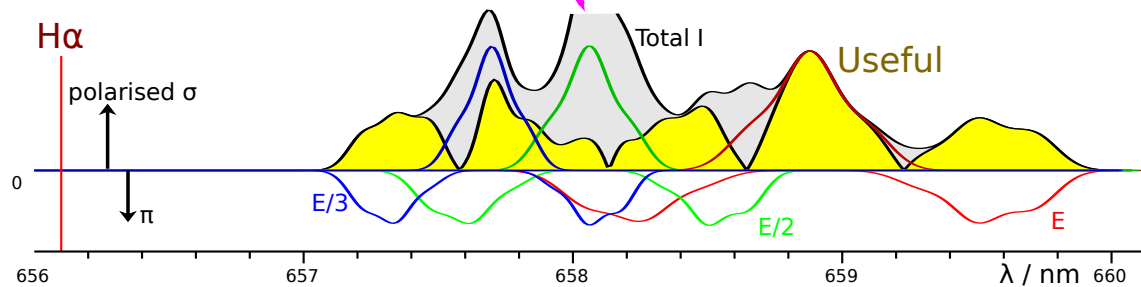
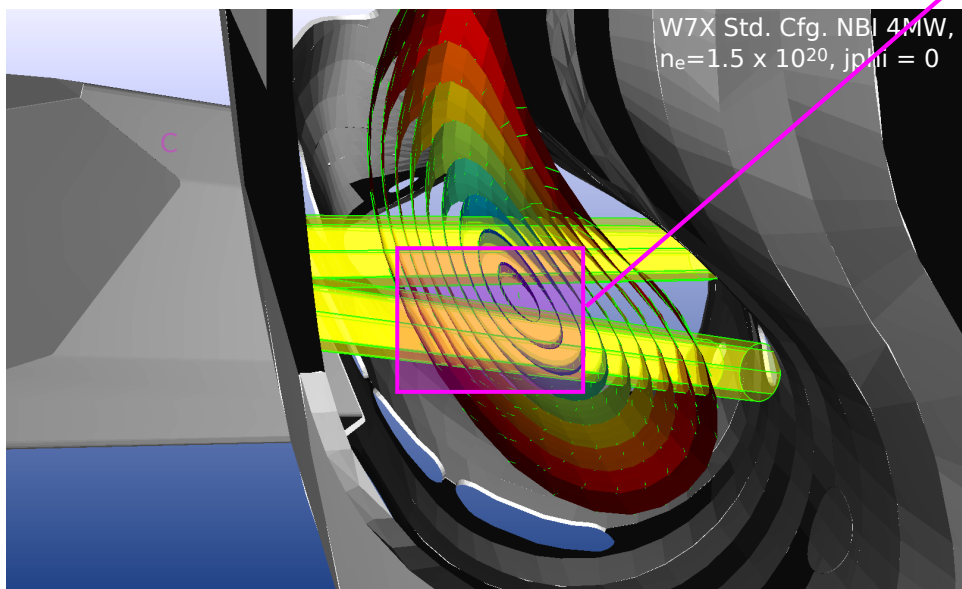
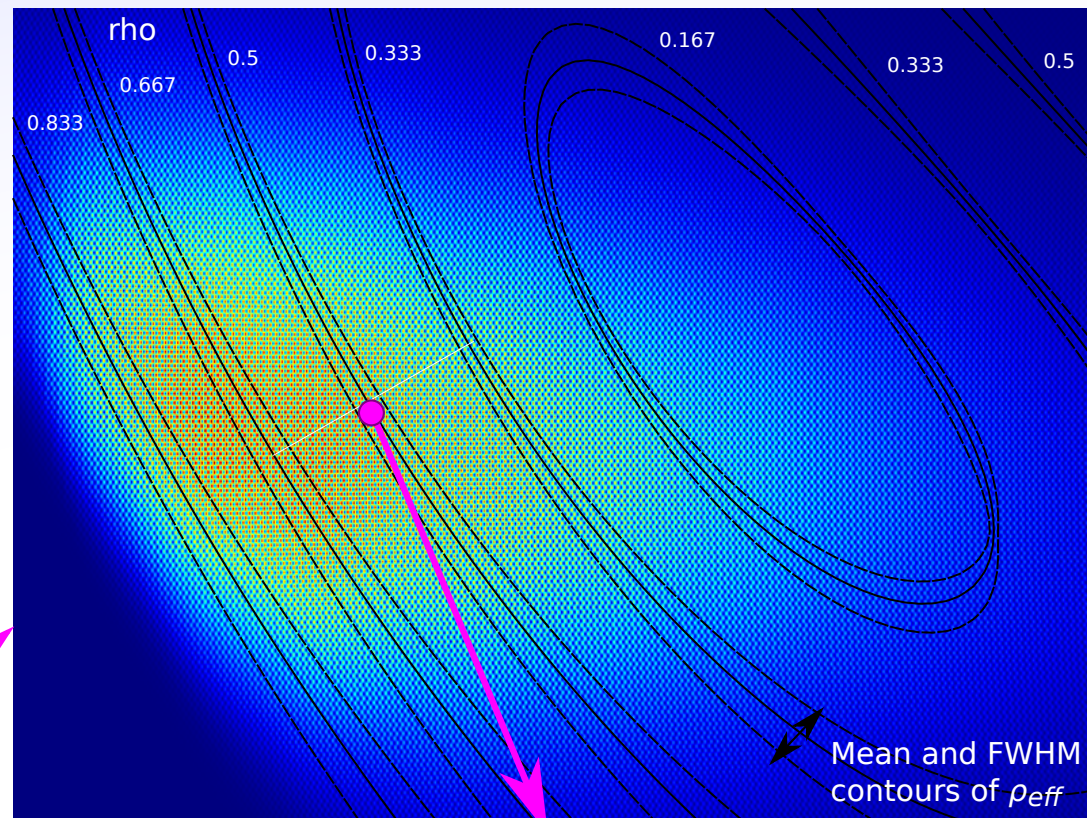
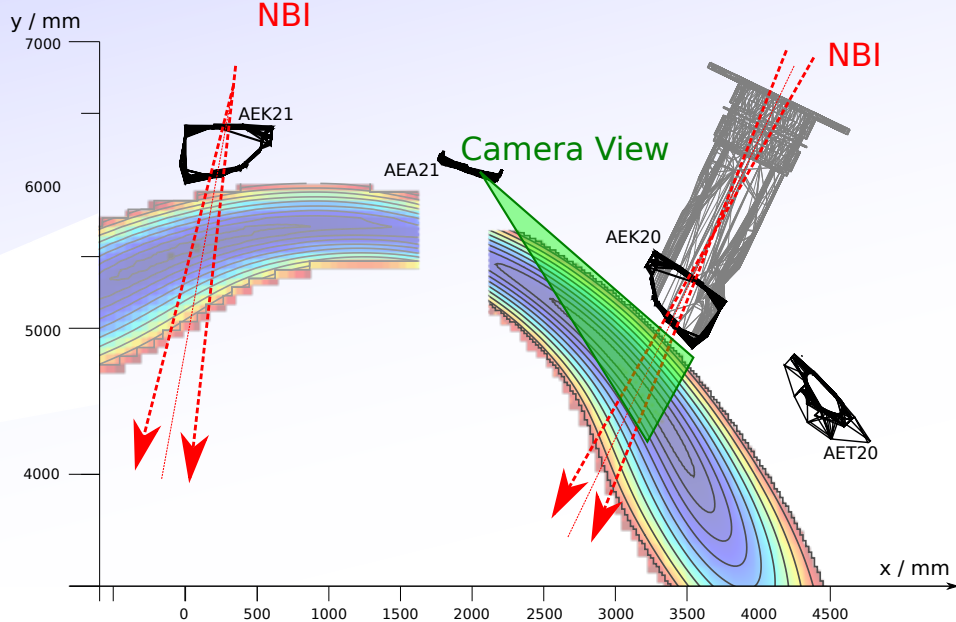




# Geometry (W7X)



A port in between the two NBI boxes is available for the CXRS and MSE systems which gives good spatial resolution.

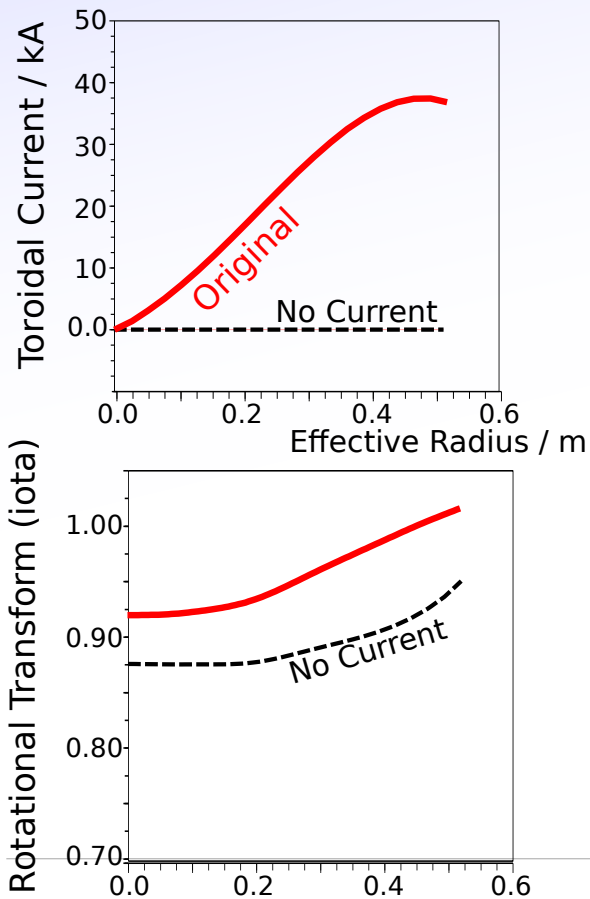


Spectrum and resolution are good but some extra complexity is introduced by the change in pitch angle *within* the surface.

## Inference of $j_\phi$ (W7X)

Can't do the current tomography in 3D (at present).

For a rough idea of the inference capability - use Function Parameterisation in forward model.  
Assume fixed/known pressure and coil currents and invert 40x30 polarisation angle map to  $j_\phi$ ,  
assuming the demodulation will be as good as at ASDEX Upgrade.

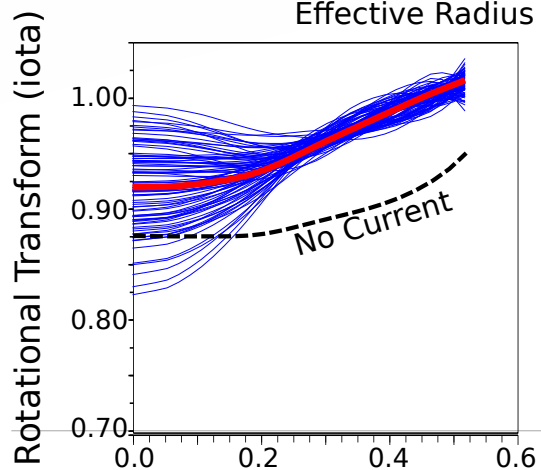
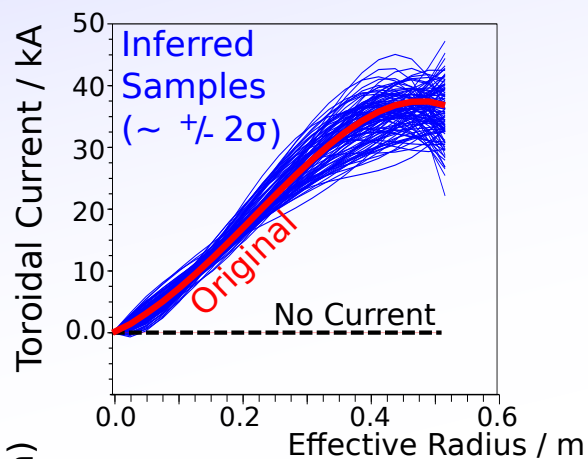




# Inference of $j_\phi$ (W7X)

Can't do the current tomography in 3D (at present).

For a rough idea of the inference capability - use Function Parameterisation in forward model.  
Assume fixed/known pressure and coil currents and invert 40x30 polarisation angle map to  $j_\phi$ , assuming the demodulation will be as good as at ASDEX Upgrade.



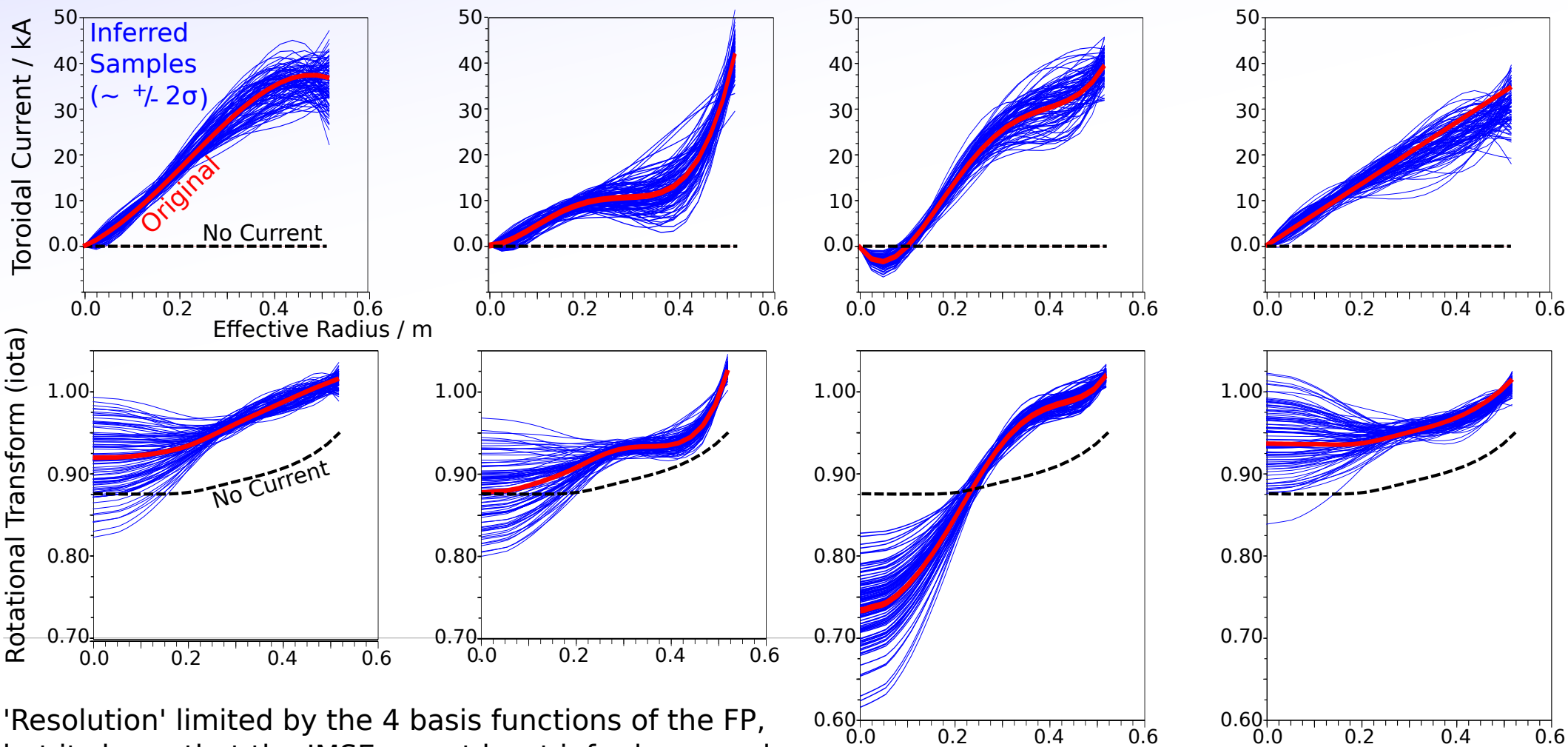


# Inference of $j_\phi$ (W7X)

Can't do the current tomography in 3D (at present).

For a rough idea of the inference capability - use Function Parameterisation in forward model.

Assume fixed/known pressure and coil currents and invert 40x30 polarisation angle map to  $j_\phi$ , assuming the demodulation will be as good as at ASDEX Upgrade.



'Resolution' limited by the 4 basis functions of the FP, but it shows that the IMSE can at least infer large scale properties of the bootstrap current profile.

Including other magnetic diagnostics should improve this further.



# Summary

## Conclusions:

- ✓ 2D MSE measurements increase the data quantity and also the information per data point.
- ✓ An IMSE diagnostic has been designed, constructed and operated at ASDEX Upgrade.
- ✓ Polarisation angle images were recorded over two periods with Hydrogen and Deuterium beams.
- ✓ Initial analysis shows agreement with conventional MSE for a repeated plasma.
- ✓ Forward modelling shows agreement with expected polarisation well within expected uncertainty, implying no significant effects in forward optics are missing from the model.
- ✓ Evaluation of different beams confirms measurement linearity and provides a cross-check of pitch angle when absolute calibration is unavailable.
- ✓ Initial modelling for W7X shows an IMSE system can provide measurement of the bootstrap current.



# Summary

## Conclusions:

- ✓ 2D MSE measurements increase the data quantity and also the information per data point.
- ✓ An IMSE diagnostic has been designed, constructed and operated at ASDEX Upgrade.
- ✓ Polarisation angle images were recorded over two periods with Hydrogen and Deuterium beams.
- ✓ Initial analysis shows agreement with conventional MSE for a repeated plasma.
- ✓ Forward modelling shows agreement with expected polarisation well within expected uncertainty, implying no significant effects in forward optics are missing from the model.
- ✓ Evaluation of different beams confirms measurement linearity and provides a cross-check of pitch angle when absolute calibration is unavailable.
- ✓ Initial modelling for W7X shows an IMSE system can provide measurement of the bootstrap current.

## Next steps:

- Analysis of data with Current Tomography ( $\pm$ equilibrium assumption).
- Further improvements to signal/noise, temporal resolution.
- A calibration method is required to determine the single fixed offset with  $\sim 0.1^\circ$  precision.
- Further investigation of the application of IMSE to W7X.